DEPARTMENT OF ONCOLOGY AND PATHOLOGY
Karolinska Institutet, Stockholm, Sweden

STEREOTACTIC BODY RADIATION THERAPY OF LUNG TUMOURS – CLINICAL AND DOSIMETRIC ASPECTS

Kristin Karlsson

Karolinska Institutet

Stockholm 2016

Published by Karolinska Institutet.
Printed by Eprint AB 2016

ISBN 978-91-7676-322-3

Stereotactic Body Radiation Therapy of Lung Tumours – Clinical and Dosimetric Aspects

THESIS FOR DOCTORAL DEGREE (Ph.D.)

By

Kristin Karlsson

Principal Supervisor:
Ingmar Lax, PhD, Associate Professor
Karolinska Institutet
Department of Oncology-Pathology
Division of Medical Physics

Co-supervisors:
Gavin Poludniowski, PhD
Karolinska Institutet
Department of Oncology-Pathology
Division of Medical Physics

Peter Wersäll, MD, PhD, Associate Professor
Karolinska Institutet
Department of Oncology-Pathology
Division of Oncology

Jan Nyman, MD, PhD, Associate Professor
Gothenburg University
Department of Clinical sciences
Division of Oncology

Opponent:
Dirk Verellen, PhD, Professor
Vrije Universiteit Brussel
Department of Medecine and Pharmacy
Division of Translational Radiation Oncology and Physics

Examination Board:
Anders Montelius, PhD, Associate Professor
Uppsala University
Department of Immunology, Genetics and Pathology
Division of Medical Radiation Science

Claes Mercke, MD, PhD, Professor
Karolinska Institutet
Department of Oncology-Pathology
Division of Oncology

Anders Ahnesjö, PhD, Professor
Uppsala University
Department of Immunology, Genetics and Pathology
Division of Medical Radiation Science

To all patients who have contributed,

and to those who might benefit

Abstract

The general aim of this thesis was to increase the knowledge regarding some clinical and methodological aspects, relevant in view of toxicity as well as tumour control, in stereotactic body radiation therapy (SBRT) of lung tumours. In the first two studies, reirradiation and radiation-induced atelectasis were studied. In the following two studies, estimations of doses delivered to the tumour, considering geometrical uncertainties, were performed.

Considering the very high biological tumour doses delivered in SBRT, knowledge of the risk of high grade toxicity is of utmost importance for its clinical use. In the first study, reirradiation with SBRT of lung tumours after previous SBRT in the same region was retrospectively evaluated in 29 patients with 32 tumours with regard to toxicity, local control and survival. Larger tumour volumes and central location were correlated to more severe toxicity, and larger tumour volumes were also correlated to worse local control. Three of the patients with centrally located lung tumours died due to bleeding, while no grade-5 toxicity was observed for patients with peripherally located tumours. The one- and three-year survival from time of reirradiation was estimated to 59% and 23%, respectively. It was concluded that reirradiation with SBRT in a location previously treated with SBRT was feasible with low rates of toxicity for patient with peripheral lung tumours, while caution should be taken for patients with central lung tumours due to the risk of increased severe toxicity.

In the second study a possible dose-response relationship for radiation-induced atelectasis and bronchial doses after SBRT close to the main, lobar or segmental bronchi was evaluated. Out of the 74 patients, 18 (24%) developed radiation-induced atelectasis at a median time of 8 month after radiotherapy. A significant dose-response relationship was found between the high-dose bronchial volume and the incidence of atelectasis. The median of the minimum dose to 0.1 cm^3 of the bronchi receiving the highest dose ($D_{0.1cm3}$) was 210 Gy_3 (EQD_2, using α/β=3 Gy) for patients with atelectasis, and 105 Gy_3 for patients without. The estimated incidence of atelectasis at 1, 2 and 3 years was 3%, 8% and 13%, respectively, at a bronchial $D_{0.1cm3}$ of 100 Gy_3, 10%, 21% and 31% at 150 Gy_3, and 25%, 42% and 53%, respectively, at a dose of 200 Gy_3.

Of decisive importance for the clinical use of SBRT is the balance between the risk of toxicity and the gain expected by control of the treated tumour. As a surrogate, to quantitatively foresee the latter, dose to the tumour is used. As planned and delivered dose may differ more in SBRT as compared to conventional radiotherapy, knowledge of delivered dose is highly important for SBRT. Study three and four were focused on the issue of delivered tumour dose in SBRT.

Study three aimed to evaluate the accuracy of a dose-shift approximation used for estimating delivered clinical target volume (CTV) doses, given the geometrical uncertainties pertinent to SBRT. For a set of 10 representative patients with lung tumours, the static dose matrix was

shifted according to clinically representative setup errors and a breathing trace scaled with different breathing amplitudes. The dose-shift approximation was compared to the more accurate beam-shift method with recalculation of dose at every geometrical position. Averaged over the patients, the disagreement between the methods for minimum CTV dose ($D_{98\%}$) was approximately 4% (root-mean-square) for setup shifts up to 10 mm, and for setup shifts up to 5 mm the disagreement was approximately 2%. It was concluded that for estimation of delivered dose for a particular patient it is advisable to use the beam-shift method for increased accuracy, while averaged over a group of patients the dose-shift approximation has an acceptable error.

In study four, the delivered CTV dose was estimated for a cohort of patients treated with SBRT, taking clinical data of breathing motions and setup errors into account. Two different volumetric soft-tissue image-guidance techniques were compared; pre-treatment verification computed tomography (CT) (IG1) and online verification with cone-beam CT (CBCT) (IG2). Treatment plans for 50 consecutively treated patients, with 69 lung tumours, were retrospectively simulated. The dose-shift approximation was used with the static dose distribution shifted according to a breathing trace scaled with patient-specific amplitudes. Applied were also systematic and random setup errors (for IG1) and matching errors (for IG2), sampled from normal distributions. Each simulation was repeated 500 times for each tumour. For each tumour, 500 different dose-volume histograms were obtained, and from those a tumour-specific dose coverage histogram was calculated. For all tumours, a population-averaged dose coverage histogram was calculated as the mean of the tumour-specific dose coverage histograms. The result showed that prescribed dose, to the periphery of the planning target volume, was delivered to 98% of the CTV with a population coverage probability within 86-96% (range between worst and best case setup assumptions, realistic assumptions: 90%) using IG1, and 97-99% (realistic assumptions: 99%) using IG2. Looking at 90% of the simulations with highest dose to 98% of the CTV (tumour coverage probability), at least the prescribed dose was delivered to 67% of the tumours with IG1 using realistic assumptions of setup errors, and to 99% of the tumours with IG2. In conclusion, the minimum dose delivered to the CTV increased with the use of online CBCT image-guidance, compared to the pre-treatment verification CT.

Populärvetenskaplig sammanfattning

Lungcancer är den femte vanligaste cancerformen i Sverige och orsakar mest cancerrelaterad död med en 5-årsöverlevnad på 15%. Detta beror delvis på att mer än hälften av patienterna har spridd sjukdom vid diagnos, cirka en tredjedel har lokalt avancerad sjukdom, och bara en femtedel upptäcks med lokaliserad lungtumör. För de senare är kirurgi förstahandsalternativet för behandling, men många patienter är medicinskt inoperabla, dvs inte kandidater för kirurgi, på grund av samsjuklighet eller för dålig lungfunktion. Då kan stereotaktisk strålbehandling (SBRT) med hög precision och få behandlingstillfällen framgångsrikt användas, med möjlighet att uppnå lokal kontroll. Denna metod kan också användas vid enstaka lungmetastas från annan cancersjukdom. Syftet med denna avhandling var att öka kunskapen kring några av de frågeställningar vi ställs inför i den dagliga verksamheten inom SBRT av lungtumörer.

Med allt bättre behandlingsresultat och allt längre överlevnad efter cancerdiagnos ökar antalet patienter som behöver upprepad behandling. I den första studien undersöktes möjligheterna till rebestrålning med SBRT efter tidigare SBRT i samma område, främst med avseende på biverkningar. Slutsatsen var att rebestrålning med SBRT är möjlig med acceptabla nivåer av biverkningar för patienter med icke-centralt belägna lungtumörer. För patienter med centralt belägna lungtumörer bör man vara extra försiktig, då högre risk för allvarliga biverkningar observerades för dessa.

Tumörer belägna centralt i lungorna, nära strålkänsliga riskorgan så som luftvägarna, är svåra att behandla. I den andra studien analyserades förhållandet mellan strålningsinducerad kollaps av hela eller del av lungan (atelektas) och doser till luftvägarna vid SBRT. Ett förhållande hittades mellan uppkomsten av lungkollaps och dosen till högdosområdet av luftvägarna.

Att uppskatta den dos som faktiskt ges till tumören vid SBRT utifrån den dos som är planerad är viktigt för att bättre kunna förstå sambandet mellan dosen och sannolikheten att få kontroll på tumören. I den tredje studien undersöks noggrannheten i en enklare och snabbare metod för att uppskatta given dos, med hänsyn tagen till andningsrörelser och positioneringsvariationer vid behandlingen. Den enklare metoden, som innebär att den statistiska dosfördelningen förflyttas, jämförs med en noggrannare metod, där behandlingsfälten förflyttas och dosen räknas om i varje geometrisk position. Slutsatsen var att den enklare metoden generellt sett uppskattade en lägre tumördos i jämförelse med den noggrannare metoden. Men vid realistiska antaganden om osäkerheter och sett för en hel grupp av patienter var skillnaden begränsad mellan metoderna.

I den fjärde studien användes ovannämnda enklare metod för att uppskatta given tumördos för en grupp patienter med lungtumörer behandlade med SBRT. Då den tekniska utvecklingen inom strålbehandling har varit stor de senaste decennierna så jämfördes given dos vid behandling med användandet av två olika bildtagningsmetoder för ökad positioneringsprecision. Slutsatsen var att den dos som ordinerades till tumören i högre utsträckning gavs vid behandling med hjälp av den nyare bildtagningstekniken.

List of scientific papers

I. Peulen H, KARLSSON K, Lindberg K, Tullgren O, Baumann P, Lax I, Lewensohn R, and Wersäll P. Toxicity after reirradiation of pulmonary tumours with stereotactic body radiotherapy. *Radiotherapy and Oncology* 2011;101:260-266.

II. KARLSSON K, Nyman J, Baumann P, Wersäll P, Drugge N, Gagliardi G, Johansson KA, Persson JO, Rutkowska E, Tullgren O, and Lax I. Retrospective cohort study of bronchial doses and radiation-induced atelectasis after stereotactic body radiation therapy of lung tumors located close to the bronchial tree. *International Journal of Radiation Oncology Biology Physics* 2013;87:590-595.

III. KARLSSON K, Lax I, Lindbäck E, and Poludniowski G. Accuracy of the dose-shift approximation in estimating the delivered dose in SBRT of lung tumours considering setup errors and breathing motions. *Manuscript*.

IV. KARLSSON K, Lax I, Lindbäck E, Wersäll P, Lindberg K, and Poludniowski G. Estimation of delivered dose to lung tumours considering setup uncertainties and breathing motion in a cohort of patients treated with SBRT. *Manuscript*.

Contents

List of abbreviations

3D	Three-Dimensional
4D	Four-Dimensional
4DCT	Four-Dimensional Computed Tomography
AAA	Analytical Anisotropic Algorithm
ADL	Activities of Daily Living
AUC	Area Under the Curve
BED	Biologically Effective Dose
BED_{10}	Biologically Effective Dose, using α/β=10 Gy
BSh	Beam-Shift
CBCT	Cone-Beam Computed Tomography
CC	Collapsed Cone
COPD	Chronic Obstructive Pulmonary Disease
CR	Complete Response
CT	Computed Tomography
CTCAE	Common Terminology Criteria for Adverse Events
CTV	Clinical Target Volume
CVD	Cardiovascular diseases
d	Fraction dose
D	Total dose
D_x	Minimum dose to volume x receiving the highest dose
DNA	Deoxyribonucleic acid
DSh	Dose-Shift
DVH	Dose-Volume Histogram
EQD_2	Equivalent Dose in 2 Gy fractions
FFLR	Freedom From Local Recurrence
FFLP	Freedom From Local Progression
FSU	Functional Subunit
GTV	Gross Tumour Volume
Gy_3	Gray, using α/β=3 Gy
Gy_{10}	Gray, using α/β=10 Gy
ICRU	International Commission of Radiation Units & Measurements
IGRT	Image-Guided Radiation Therapy
ITV	Internal Target Volume
LC	Local Control
LR	Local Recurrence/Relapse
LQ	Linear Quadratic
MC	Monte Carlo
MLC	Multi-Leaf Collimation
MLD	Mean Lung Dose
MR	Magnetic Resonance
n	Number of fractions
NSCLC	Non-Small Cell Lung Cancer
NTCP	Normal Tissue Complication Probability
OAR	Organs At Risk

OS	Overall Survival
PB	Pencil Beam
PD	Progressive Disease
PET	Positron Emission Tomography
PR	Partial Response
PTV	Planning Target Volume
RECIST	Response Evaluation Criteria In Solid Tumours
ROC	Receiver Operating Characteristic
RT	Radiation Therapy
SBF	Stereotactic Body Frame
SBRT	Stereotactic Body Radiation Therapy
SD	Stable Disease
SF	Surviving Fraction
SRT	Stereotactic Radiation Therapy
std	Standard Deviation
TCP	Tumour Control Probability
TPS	Treatment Planning System
USC	Universal Survival Curve
V_x	Volume receiving at least dose x
VMAT	Volumetric Modulated Arc Therapy

1 Introduction

1.1 Lung cancer

Current statistics about the prevalence, prognosis and treatment strategies for lung cancer in Sweden are published by Socialstyrelsen, Cancerfonden and Regionala Cancercentrum i Samverkan (Regionala Cancercentrum i Samverkan, 2015; Socialstyrelsen, 2015; Socialstyrelsen & Cancerfonden, 2013). It is estimated that about every 3rd person in Sweden will have a cancer diagnosis during their lifetime. About 50,000 persons are newly diagnosed with cancer each year, and the survival rate averaged over all cancer diagnoses is about 70% at 5 years after diagnosis, and about 65% at 10 years. Lung cancer is the 5th most common cancer in Sweden but is the most common cause of cancer-related death, both among men and women. The survival rate is about 15% at 5 years after diagnosis, and about 10% at 10 years. The poor survival is due to the commonly late discovery of lung cancer, high age at diagnosis and concomitant comorbidities, which limits the treatment possibilities. Besides the primary lung tumours, included in the term *lung tumours* are also lung metastases. Lung metastases are common from several cancer diagnoses including primary lung cancer, but also diagnoses such as colorectal cancer and renal cancer.

The first choice of treatment for localised lung tumours (Stage I-II) is surgery, commonly by removing the lung lobe or a wedge of the lobe where the tumour is located, which is possible in less than 20% of newly diagnosed patients. If the patient is inoperable due to reduced general medical condition or comorbidities, like chronic obstructive pulmonary disease (COPD) or cardiovascular diseases (CVD), the patient could be referred to local treatment with radiotherapy (RT).

1.2 Conventional radiotherapy

Most commonly lung cancer is diagnosed at a late stage of the disease. Approximately one-third of the patients are diagnosed with locally advanced disease with lymph node involvement (Stage III). For some of these patients, treatment with combined chemo- and radiotherapy with curative intent is possible. The extent of the disease might lead to high doses to adjacent organs at risk, with increased risk of different kinds of toxicity. However, more than half of the patients are diagnosed with distant metastases (Stage IV), where chemotherapy is the primary choice. Some of these patients are treated with radiotherapy in a palliative setting for relief of pain, dyspnea, hemoptysis etc.

To facilitate consistent reporting of dose to the tumour and surrounding normal tissues and healthy organs in radiotherapy, relevant structures to be delineated during treatment planning are defined by the International Commission of Radiation Units & Measurements (ICRU) in reports 50, 62 and 83 (ICRU, 1993, 1999, 2010) as follows:

- Gross tumour volume (GTV) – The visible or palpable extent and location of tumour growth: this might be primary tumour, metastasis or metastatic nodes
- Clinical target volume (CTV) – This includes the GTV and microscopic or subclinical tumour cells, or diffuse and spiky growth around the GTV; it is defined by clinical experience
- Internal target volume (ITV) – This accounts for variations in size, shape and position of the CTV; it is defined typically by recording the breathing motion
- Planning target volume (PTV) – This includes the CTV (or the ITV) with the addition of a margin to account for the total effect of all relevant geometrical and dosimetric uncertainties; the target dose is typically specified to this volume, to ensure acceptable probability of the delivery of prescribed dose to the CTV
- Organs at risk (OAR) – These are the selected normal tissues that due to their sensitivity to radiation might affect the treatment planning or the prescribed dose

In conventional radiotherapy, the dose distribution is planned to be homogeneous within the tumour region. Often 95% of the prescribed dose is planned to cover the PTV, but sometimes with a trade-off between target coverage (probability for local control) and the dose to organs at risk (risk of side-effects).

Clinical experience obtained early in the history of radiotherapy showed that dividing the treatment into multiple fractions could result in tumour control but with less severe side-effects compared to a single fraction. This was later explained by radiobiological research. Normal tissue cells generally have a better ability to repair damage than most cancer cells (Steel & Nahum, 2007), implying fractionated radiotherapy to be more gentle for the normal cells without losing too much therapeutic effect on the cancer cells. Lower dose per fraction is beneficial for recovery of late-responding normal tissues (Steel & Nahum, 2007). However, there is a benefit of shortening the overall treatment time to reduce proliferation of tumour cells during the treatment (Steel & Nahum, 2007). In external beam radiotherapy the general convention today is to prescribe 2 Gy per fraction to the tumour, given in daily weekday fractions during several weeks. However, there are also other kinds of treatment schedules like accelerated hyperfractionated treatments with lower dose per fraction delivered in a shorter overall treatment time, and hypofractionated treatments with higher dose per fraction delivered in fewer fractions. The appropriate treatment schedule can vary depending on the patient, cancer type, body site and intent of therapy, *e.g.* curative or palliative therapy.

1.3 Stereotactic body radiation therapy

With the implementation in clinical practice of computed tomography (CT), multi-leaf collimators (MLCs) and 3D treatment planning, it became possible to obtain high conformity of the dose distribution to the PTV. This led to the possibility to decrease the dose to OAR, and due to that the possibility of hypofractionation, despite the apparent radiobiological disadvantage. Hypofractionation is one of the key aspects of stereotactic treatments.

The concept of stereotactic treatments started with intracranial stereotactic radiation therapy (SRT) developed from the 1950s by Lars Leksell. The Gamma Knife has been used in clinical practice since 1968 (Lax & Blomgren, 2005; Leksell, 1983). This treatment unit has about 200 Cobalt-60 sources placed in a hemispherical shape to treat brain tumours or malfunctions with a very high dose delivered in a single treatment fraction. The dose distribution is heterogeneous within the target volume for two reasons. The first is that the highest possible dose gradient was intended at the periphery of the target. The second is related to the way the total dose distribution was built up from several almost spherical high-dose volumes, called shots. The high geometrical accuracy in the dose delivery in SRT was based on the use of a rigid stereotactic frame placed with screws into the skull bone as an external reference system. The outcome of these treatments has been very good with high local control rates and low toxicity for selected targets (Lax & Blomgren, 2005; Leksell, 1983).

The idea of extending this way of treating tumours to targets located in the thorax and abdomen led to the development of stereotactic body radiation therapy (SBRT) in the early 1990s (Lax & Blomgren, 2005; Lax, Blomgren, Näslund, & Svanström, 1994). SBRT with hypofractionation started with relatively small tumours in the liver and lungs, and required a high geometrical accuracy of the treatment delivery. Essential aspects considered were, among others, the concept of tumour localisation with a stereotactic coordinate system, rigid patient immobilisation, heterogeneity of the dose distribution and hypofractionated regimen. For patients considered inoperable with localised primary lung tumours, or one or a few lung metastases from other cancer diagnoses, SBRT can be used with possibilities to achieve local tumour control.

1.4 Purpose of this thesis

The purpose of this thesis was to increase the knowledge regarding some of the considerations in daily clinical practice that need to be solved in SBRT of lung tumours, in order to improve this technique and to extend the scope of it to cases not previously considered, through the implementation of modern technologies and clinical experience collected in our clinic and elsewhere.

Paper I. The first question to be answered was the feasibility of using SBRT for reirradiation of lung tumours in patients already treated with SBRT in the same region. In lack of other efficient treatment options for these patients, it was of utmost importance to evaluate the possibilities of treatment with this technique. A retrospective review of medical records and treatment plans were conducted, primarily evaluating toxicity (Peulen *et al*., 2011).

Paper II. The second question to be investigated was the tolerance dose of the bronchial tree at SBRT. Several cases of radiation-induced atelectasis had been observed after SBRT of tumours close to the bronchi. The aim of the study was to estimate the relationship between

radiation-induced atelectasis and doses to the bronchi (Karlsson *et al*., 2013). The incidence of radiation-induced atelectasis was retrospectively evaluated from medical records and the relationship with planned bronchial doses was subsequently modelled.

Papers III and IV. The third question to be investigated was that of the actual dose delivered (rather than planned) to lung tumours with SBRT, considering geometrical uncertainties. This was thought to be an issue of importance especially due to the form of the dose distributions used in SBRT and their impact under breathing motion and setup errors. The aim was to evaluate the dose delivered to the tumour to be able to explore the possibility of reducing the CTV-to-PTV margins while maintaining the high local tumour control, with the prospect of reduced toxicity. In Paper III the accuracy of a dose-shift (DSh) approximation was evaluated, modelling setup errors and breathing motions by shifting the static invariant dose distribution. This approach was compared to a beam-shift (BSh) model, simulating the same setup errors and breathing motions but with shifts of the beams/isocenter and recalculation of the dose distribution at each geometrical position. In Paper IV the DSh model was used to estimate the delivered dose considering setup uncertainties and breathing motions, comparing two different soft-tissue image-guidance techniques; pre-treatment verification CT (IG1) and online cone-beam CT (CBCT) (IG2). The delivered dose was estimated in terms of coverage probability of the CTV (to be covered by a certain dose), with tumour coverage probability for a single tumour and population coverage probability averaged over a population of tumours.

In Chapter 2, the radiation physics and biology underpinning radiotherapy and SBRT is described. The methodological aspects of delivering SBRT are elaborated upon in Chapter 3. In Chapter 4, the clinical aspects providing context to the projects are presented. In Chapter 5, the geometric and dosimetric aspects of planning and delivery of SBRT are summarised, providing the context for the work presented in Paper III and IV. Chapter 6 summarises in detail the papers that constitute this thesis. Finally, Chapter 7 summarises the main conclusions and Chapter 8 highlights some possibilities for future research.

2 Radiation physics and biology

2.1 Radiation interaction

Megavoltage photons are the most common radiotherapy modality. The main mechanisms for energy deposition of photon interactions are the photoelectric effect, Compton scatter, pair production and photonuclear reactions (Nikjoo, Uehara, & Emfietzoglou, 2012). Compton scatter is the dominating interaction process at photon energies between 100 keV-20 MeV in low atomic number materials (Dance & Alm Carlsson, 2007), which is the case in RT of humans. In this interaction process, the incident photon interacts with a free or atomic electron, and the photon and the secondary electron are scattered in different directions. The photon can be scattered in all angles, while the secondary electron is scattered in forward angles (Dance & Alm Carlsson, 2007; Nikjoo *et al*., 2012). The higher the incoming photon energy, the more forward-focused the scattering distribution of the photon, and the higher the energy transferred to the electron (Dance & Alm Carlsson, 2007). For a 6 MV beam the range of the Compton electrons will be around 16 mm in human tissues (Mayles & Williams, 2007), while the scattered photons reach much farther (Dance & Alm Carlsson, 2007). The scattered photons and electrons continue to interact with the surrounding tissues in several generations. Most of the energy loss events of the Compton scattered electrons occur through soft collisions, with small energy transfer, when the electron passes an atom at a distance and affects the whole atom by excitation or ionisation of an outer-shell electron (Nahum, 2007). When the electron passes an atom at a close distance, a hard collision may occur where a larger amount of energy is transferred to one of the atomic electrons that is ejected, called a delta-ray (Nahum, 2007).

This chain reaction of photons and electrons results in ionisations and excitations of the atoms in the cells (Nikjoo *et al*., 2012; Steel, Chapman, & Nahum, 2007). The interactions in human tissues occur mainly with water, but also with lipids, proteins and the deoxyribonucleic acid (DNA) (Okunieff, 2005). In contrast to most components of a cell, the DNA chain has no redundancy; its unique encoding of genes with essential functions, which makes the impact of DNA damage much more severe (Steel *et al*., 2007; Wouters & Begg, 2009). About 70% of the biological effect of the irradiated cells is caused by ionisations of the water molecules, resulting in highly reactive free radicals (Nias, 2000). The other part is due to direct damage of biological structures (Nias, 2000), by primary and secondary photons and their corresponding secondary electrons. Inside the cell there are many enzymes to repair DNA damage, which occur spontaneously on average tens of thousands of times in a human cell during a day (Bernstein, Prasad, Nfonsam, & Bernstein, 2013). However, the damage can also be lethal, *i.e.* leading to apoptosis or necrosis within hours, or cause mutations leading to cancer after many years, or hereditary damage in coming generations. Besides the DNA damage, signalling proteins (cytokines) are produced within the irradiated region (Okunieff, 2005). These cytokines can for example induce apoptosis, necrosis, proliferation, cell cycle

arrest and promote or inhibit inflammation, and are a large cause of the indirect consequences of radiation leading to late effects (Okunieff, 2005).

The purpose of radiotherapy is to prevent proliferation (mitosis) of the tumour cells so that the cells lose their ability to form colonies of cells, known as proliferative cell death, or to induce apoptosis (Hagan, Yacoub, Grant, & Dent, 2005; Okunieff, 2005; Steel *et al.*, 2007), without causing too much irreparable damage to normal cells. The absorbed dose in tissue correlates with the damage of the cells (Steel, 2007). Photon irradiation with 1 Gy gives about 100,000-200,000 ionisations in every cell nucleus (Steel *et al.*, 2007), leading to about 1000 or even up to 20,000 single-strand breaks and 20-40 double-strand breaks of the DNA (Okunieff, 2005; Steel *et al.*, 2007; Wouters & Begg, 2009). Single-strand breaks are easily repaired, while double-strand breaks are a more serious type of damage. Despite such extensive damage at 1 Gy, the effective repair enzymes enable most cells to survive anyway (Steel *et al.*, 2007), resulting in about 30% cell kill in human cells (Wouters & Begg, 2009). However, most cancer cells are less effective in repairing damage than normal cells are (Steel & Nahum, 2007).

2.2 Radiobiological models

To model cell survival, the term *surviving fraction* is used which is defined in cell-studies as the number of irradiated cells with preserved reproductive (mitotic) function and ability to form colonies compared to the number of the non-irradiated cells (Steel *et al.*, 2007). Besides the loss of reproductive function, irradiation may also lead to smaller colony sizes or reduced growth rate of cell colonies, not generally considered in radiobiological models evaluating the radiation effect (Steel *et al.*, 2007). The relationships between the surviving fraction and the radiation dose (absorbed dose) are plotted in cell survival curves (Figure 1).

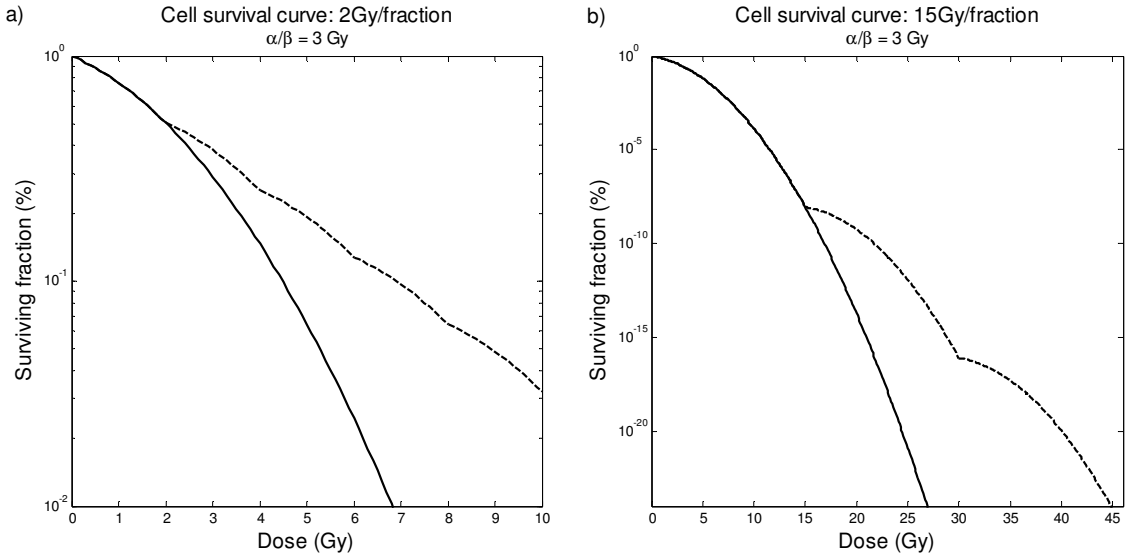

***Figure 1**: Cell survival curves with surviving fraction on logarithmic scale, for single fraction (solid line) and multiple a) 2 Gy/fraction and b) 15 Gy/fraction (dashed line), calculated with the LQ model, using α/β=3 Gy, and α=0.206 Gy^{-1} from Wennberg and Lax (2013) for normal tissues.*

Whether every single tumour cell has to be killed to achieve local tumour control has been debated and studied over the years, but there are no results supporting the opposite and no consensus has yet been reached (Steel *et al*., 2007).

An essential factor affecting the cell survival is the fractionation schedule. The different important aspects of fractionation are summarised in the *5 Rs of radiotherapy*:

- **Repair** – Repair of the cells occur within a few hours after irradiation, making the tissue more radioresistant for fractionated radiotherapy (Steel *et al*., 2007).
- **Redistribution** or **Reassortment** – Redistribution of the cells in the cell cycle between fractions which increases the probability of irradiating cancer cells in a more radiosensitive phase of the cell cycle at repeated fractions, and makes the tissue more radiosensitive for fractionation (Steel *et al*., 2007).
- **Repopulation** – Repopulation rates for tumour cells are generally slow (but vary) with an average doubling time of about three months (Steel & Nahum, 2007). However, after induced damage the repopulation rate appears to increase, with doubling times shorter than one week (Steel & Nahum, 2007). Repopulation increases the tissue radioresistance at fractionated therapy (Steel *et al*., 2007).
- **Reoxygenation** – Hypoxic cells are more radioresistant, and reoxygenation of these cells makes them more radiosensitive at repeated treatment fractions (Steel *et al*., 2007). Generally, most hypoxic cells require about three times the dose as oxic cells for the same biological effect (oxygen enhancement ratio) (Fowler, Tome, & Welsh, 2005); this factor might be reduced at fraction doses below 3 Gy (Steel *et al*., 2007).
- **Radiosensitivity** – Radiosensitivity between different kinds of normal cells and cancer cells differs (Steel *et al*., 2007). Radiosensitivity is quantified as the surviving fraction at 2 Gy (SF_2).

This complex process of cell killing is challenging to describe in mathematical models. Regardless, there are several proposed radiobiological models that describe cell survival *in vitro*, which have been applied *in vivo*. The most frequently used is the linear-quadratic (LQ) model. However, it has been suggested that application of the LQ model at high fraction doses is limited, and several other models have been proposed, among which the Universal Survival Curve (USC) (Park, Papiez, Zhang, Story, & Timmerman, 2008) is one commonly used.

2.2.1 Linear-quadratic model

The LQ model of cell killing describes the logarithm of the surviving fraction (SF) of the irradiated cells as a continuous bending curve (Steel *et al*., 2007), as illustrated in Figure 1. After treatment with n number of fractions of the dose d the SF is calculated by (Steel & Nahum, 2007):

$$SF_{LQ} = \left(e^{-\alpha d - \beta d^2}\right)^n \quad (1)$$

where α describes the initial slope of the survival curve, while β describes the curvature in a semi-log plot (*c.f.* Figure 1).

The cell-specific parameters α and β may be obtained from experimental *in vitro* systems. These values may however not be relevant for *in vivo* (clinical) systems, and have to be obtained from clinical follow-up data for the end-point of interest. For the latter case the biologically effective dose (BED) can be derived from the LQ equation, recalculating the actual fractionation schedule into the equivalent dose given in infinitely small fractions (Steel & Nahum, 2007):

$$BED = nd\frac{d+\alpha/\beta}{\alpha/\beta} \quad (2)$$

where d is the dose per fraction and n is the number of fractions. Calculations of BED using α/β=10 Gy are denoted BED_{10}.

From different sets of clinical data, all with the same biological/clinical end-point (same BED), but obtained with different fractionation schedules (d, n), values for α and β may be obtained. However, accurately obtained parameter values relevant for clinical radiotherapy are sometimes hard to find, and sometimes values obtained from *in vitro* systems are used in the clinic.

The quotient between α and β parameters describes the fractionation sensitivity, where a low α/β ratio means a more curved survival curve and a greater dependence on fractionation (dose per fraction) (Steel & Nahum, 2007). It has been shown, initially from experimental animal data, that a higher fractionation sensitivity is correlated with a late radiation response (Thames & Hendry, 1987).

A generally used value for the α/β ratio in clinical practice, for tumours as well as for early responding normal tissue, is 10 Gy, even though there are exceptions with lower α/β values for some tumour types (Steel & Nahum, 2007). Late responding normal tissues are often assigned a ratio of 3 Gy. This means that a late-responding normal tissue is more affected by fractionation than tumours are, and that many small fractions are beneficial for normal tissues without any larger loss of treatment effect of the tumour.

From the LQ equation the equivalent dose in 2 Gy fractions (EQD_2) can be derived, used to recalculate a dose of *d* Gy/fraction in *n* fractions into the total dose giving the same surviving fraction as given with 2 Gy/fraction:

$$EQD_2 = nd\frac{d+\alpha/\beta}{2+\alpha/\beta} \quad (3)$$

Calculations of EQD_2 using α/β=3 Gy are denoted Gy_3 and calculations using α/β=10 Gy are denoted Gy_{10}.

2.2.2 Universal survival curve

To more accurately model the biological effect for hypofractionation with high fraction doses, the USC model has been proposed by Park *et al*. (2008). The USC model uses the LQ model at low fraction doses up to the transition dose d_T to describe the shoulder of the survival curve, and the single-hit multitarget (SHMT) model above d_T as a straight line, in a semi-log plot (see Figure 2).

The surviving fraction with the SHMT model is calculated as (Joiner, 2009; Wennberg & Lax, 2013):

$$SF_{SHMT} = \left(1 - \left(1 - e^{-d/D_0}\right)^{\bar{n}}\right)^n \quad (4)$$

where *n* is the number of fractions and *d* is the fraction dose, as in the LQ model, while D_0 is the dose that on average gives one hit per target (defined in the model as an assumption of a sensitive region of the DNA) and determines the slope ($-1/D_0$), and $\bar{n}$ is the number of targets in the cell and represents the extrapolated y-intercept of the linear part of the log-linear survival curve. At high doses the SHMT model asymptotically approaches a straight line (Wennberg & Lax, 2013):

$$\ln(SF_{SHMT}) = \left(-\frac{1}{D_0}d + \ln(\bar{n})\right) \cdot n \quad (5)$$

Comparisons of the LQ and the USC models with regard to the SF at different doses, for both tumour and normal tissue with dose delivered in 3 and 8 fractions respectively, can be seen in Figure 2. The parameter values used were, following Wennberg and Lax (2013); D_0 = 1.25 Gy, $\bar{n}$ = 4.5, d_T = 6.61 Gy, α/β = 10 Gy and α = 0.3446 Gy^{-1} (tumour), and D_0 = 1 Gy, $\bar{n}$ = 10, d_T = 5.8 Gy, α/β = 3 Gy and α = 0.206 Gy^{-1} (normal tissue).

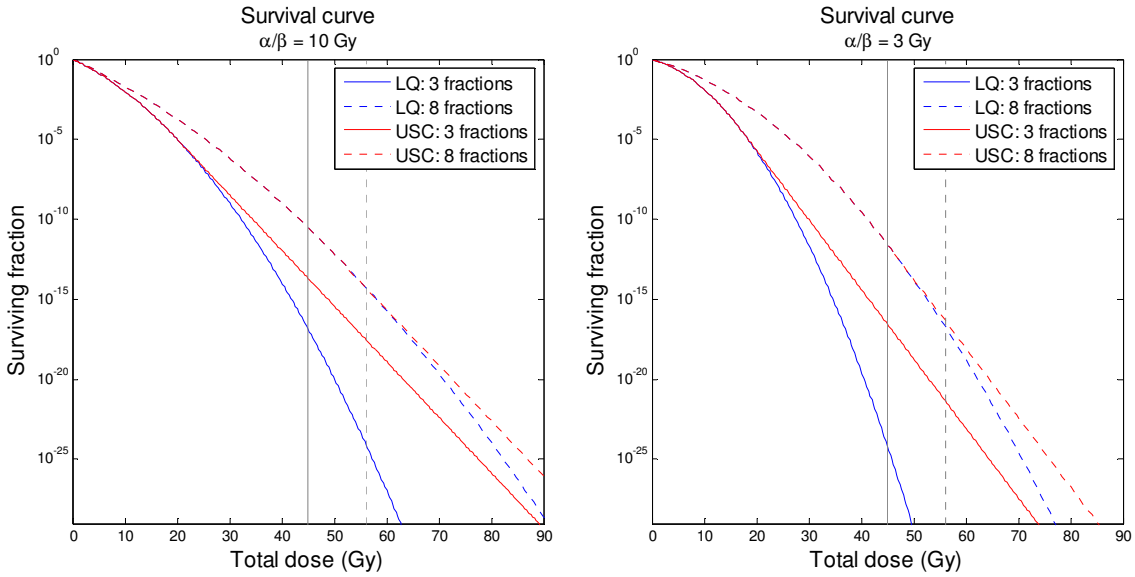

***Figure 2**: Survival curves calculated with the LQ (blue) and the USC (red) models for 3 (solid lines) and 8 (dotted lines) fractions, using α/β = 10 Gy (left) and α/β = 3 Gy (right). Indicated (grey lines) are total doses of 45 Gy (15 Gy × 3) and 56 Gy (7 Gy × 8) commonly used in our clinic.*

Figure 2 shows that there are only small differences between the LQ and the USC models for eight fractions. However, for three fractions there is a substantial difference, which is more pronounced for tissues with lower *α/β* ratios.

In Paper II, EQD_2 was calculated with both the LQ model and the USC model. The receiver operating characteristic (ROC) curves and the area under the curve (AUC) for the association between radiation-induced atelectasis and the minimum dose to 0.1 cm^3 of the bronchi receiving the highest dose ($D_{0.1cm3}$) are shown in Figure 3. No difference was shown between the two models in the predicting power of atelectasis from bronchial doses in EQD_2.

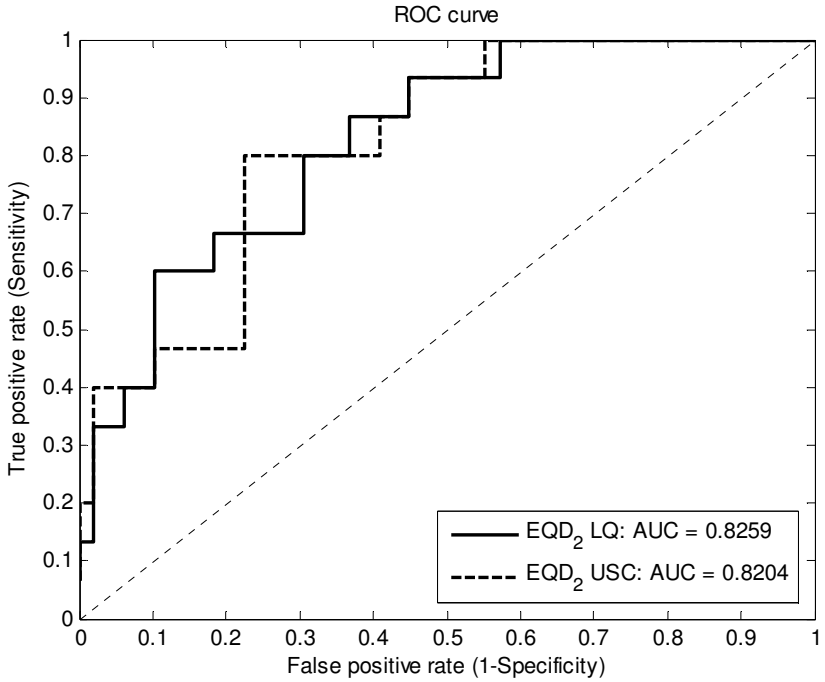

***Figure 3**: ROC curves for radiation-induced atelectasis and bronchial $D_{0.1cm3}$ in EQD_2 calculated with the LQ and USC models.*

2.3 Dose-volume response modelling

Cell survival models are commonly used in the clinic to convert doses between different fractionation schedules, by recalculating prescribed or planned doses into equivalent doses with BED or EQD_2. This is applicable for point-doses or for homogeneously irradiated tumours and organs. To get an estimate of the probability of a certain outcome after heterogeneously irradiated tumours or organs, tumour control probability (TCP) and normal tissue complication probability (NTCP) models are used. In these models, the volume effect is considered and the dose-volume histogram data for the tumour or organ is used in such a way that a single risk measure is obtained. For organs with a large functional reserve (often referred to as parallel tissues, for example, lung or liver), the mean dose is often best correlated to the end-point of interest. For organs with a small functional reserve (often referred to as serial tissues, for example, spinal cord), on the other hand, the maximum dose is often best correlated to the end-point of interest. The relationship between TCP, as well as NTCP, and dose is commonly modelled with some type of sigmoid function (see Figure 4).

The aim of radiotherapy is to treat the tumour with a dose giving a high TCP, which may be limited by the tolerance dose for normal tissues close to the tumour. The dose distribution can be optimised with regard to the therapeutic window (see Figure 4) or the therapeutic gain, *i.e.* the ratio between tumour response and normal tissue toxicity, making trade-offs between the TCP and acceptable NTCP. Whether there is a gain for the patient with increased dose depends on the steepness and the dose level, *i.e.* the location on the dose axis, of the dose-response curves for the TCP and each specific NTCP end-point, which varies depending on

different biological factors, such as the 5 Rs of radiotherapy (Steel, 2007). Generally, the dose-response curve is steeper for late-responding normal cells, than for early-responding normal cells and tumour cells (Steel, 2007). This means that the size and shape of the therapeutic window might vary for different patients, tumour types, toxicity end-points and treatment schedules.

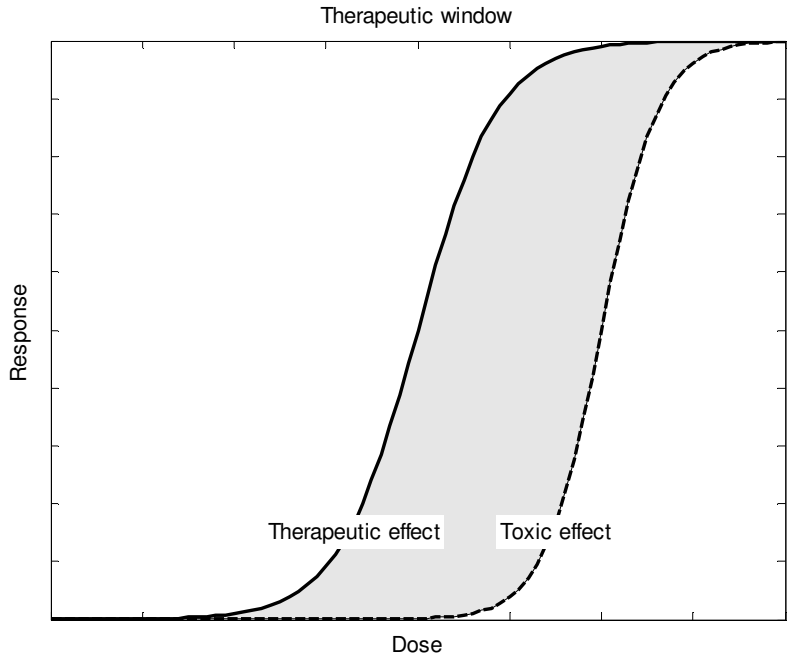

Figure 4*: Illustration of therapeutic window (grey shaded area) between sigmoid curves of therapeutic effect (TCP) and toxic effect (NTCP).*

Since cells are more or less sensitive to radiation in different phases of the cell cycle (more sensitive in G2 and mitosis phase and less sensitive in synthesis/S phase (Steel *et al*., 2007)), a result of dividing the radiotherapy dose into many fractions is that cells in a less sensitive part of the cycle at a given fraction can be in a more sensitive part at another fraction. Several factors may determine the width of the therapeutic window, such as fractionation and total treatment time (Bentzen, 2009). The former, due to the fact that normal cells are more effective in repairing damage than most cancer cells are (Steel & Nahum, 2007).

When modelling dose-response relationships the time to response and follow-up time of the patients also have to be considered. For this purpose, survival analysis models can be used. In these models, every patient contributes to the follow-up data up to the time when the studied event occurs or to the time when the patient is censored, due to becoming lost for follow-up or death caused by other reasons than the event studied (Kirkwood & Sterne, 2003). Furthermore, the risk of the event studied is not required to be constant with time, but is allowed to vary. In Paper I and II, Kaplan-Meier curves were calculated for survival and time to toxicity or atelectasis, respectively. In Paper II, also the lognormal accelerated failure time model was used, to model the dose-response relationship of radiation-induced atelectasis and bronchial doses, at different time points after treatment.

3 Methodological aspects of SBRT of lung tumours

Essential methodological aspects of SBRT were from the beginning the hypofractionated regimen, the concept of tumour localisation with a stereotactic coordinate system, rigid patient immobilisation, heterogeneity of the dose distribution, tumour position verification, the CTV-to-PTV margins and breathing motion assessment. Most of these are still essential, while some have developed over time.

3.1 SBRT at the Karolinska University Hospital

An overview of the development of the SBRT methodology at the Karolinska University Hospital over time can be seen in Table 1. In the following subsections, aspects of the methodology will be described in greater detail.

***Table 1**: A general overview of the development of the SBRT methodology at the Karolinska University Hospital over the years. Changes in treatment technique are highlighted in bold.*

Characteristics	**1991-2009**	**≥2009**	**≥2011**
Prescription isodose	~67%	~67%	~67%
Setup and fixation	SBF	SBF	SBF
Technique	Static beams	Static beams	Static beams **VMAT (2011)**
No of beams or arcs	5-7 beams	5-7 beams	5-7 beams 2-4 arcs
Photon energy	6 MV	6 MV	6 MV
Dose calculation algorithm	PB **AAA (2008)**	AAA	AAA
Geometrical verification	Verification CT	**CBCT (2009)**	CBCT
CTV definition	Tumour	Tumour	Tumour
PTV-margin (depending on breathing amplitude)	Long ≥10 mm Trans ≥5 mm	Long ≥10 mm Trans ≥5 mm	Long ≥10 mm Trans ≥5 mm
Tumour movement assessment	Diaphragm or tumour: Fluoroscopy Frontal projection	Diaphragm or tumour: Fluoroscopy **Frontal and lateral projection (2010)**	Tumour: **4DCT (2011)**

SBF = stereotactic body frame, VMAT = volumetric modulated arc therapy, PB = pencil beam, AAA = analytical anisotropic algorithm, CT = computed tomography, CBCT = cone-beam computed tomography, 4DCT = four-dimensional computed tomography

3.2 Hypofractionation

Hypofractionation, with fractionation schedules typically 10-15 Gy × 3 to the PTV periphery, was controversial when SBRT was introduced in the 1990s due to clinical practice and experience from conventionally fractionated radiotherapy. When SBRT was first introduced, the intention was to treat with single fractions, as done with the Gamma Knife, but unsatisfactory rate of local control in this early experience directed the treatment into delivering the dose in a few fractions (Blomgren, Lax, Näslund, & Svanström, 1995; Lax & Blomgren, 2005). Despite the radiobiological advantages of using many fractions,

hypofractionation in SBRT has been shown to be effective for treating certain tumours (mainly in the lungs and liver) with acceptable toxicity (Baumann *et al*., 2009; Blomgren *et al*., 1998; Blomgren *et al*., 1995). The main reasons for this appear to be the following: the selection of small tumours, the fact that the PTV only includes the gross tumour and no sensitive OAR, and the high setup accuracy allowing reduced treatment margins and consequently delivering of high tumour doses without too large doses to normal tissues. The wide acceptance of hypofractionation in SBRT today is due to the clinical results, and the practical benefit of few fractions where greater effort can be put into the tumour position reproducibility at each fraction (Lax & Blomgren, 2005).

For tumour locations close to OAR, risk-adaption of the dose prescription might, however, be necessary in order to minimise toxicity. This implies an increased number of fractions for higher-risk patients (Guckenberger, 2015). Whether that also optimises the therapeutic window, *i.e.* what consequences the increased number of fractions has on the TCP, is not yet known in detail.

In a randomised study of conventional RT (2 Gy × 35) and SBRT (15 Gy × 3 to 68% isodose encompassing the PTV) treatments of Stage I NSCLC by Nyman *et al*. (2016), no significant difference in local control (LC) was seen for the two treatment arms, at a median follow-up time of 37 months. However, lower incidence of different types of toxicity was observed within the SBRT arm, except for rib fractures. Even though the SBRT treatment is delivered in fewer fractions, the similar or lower toxicity compared to the conventional treatment might be explained by the reduced CTV-to-PTV margins used in SBRT.

Lagerwaard *et al*. report about risk-adapted SBRT fractionation schedules selected from tumour stage and risk for toxicity, with 20 Gy × 3 for T1 tumours, 12 Gy × 5 for T1 tumours with large contact (the extent of which was not specified) with the chest wall or T2 tumours, and 7.5 Gy × 8 for tumours close to the heart, hilus or mediastinum, prescribed to the 80% isodose encompassing the PTV (Lagerwaard, Haasbeek, Smit, Slotman, & Senan, 2008). They show a local progression-free survival at 1 and 2 years of 98% and 93%, respectively, and less than 3% of the patients experienced severe late toxicity (local control results were not reported). This indicates promising results with risk-adapted fractionation, however, with only a minor part of the included patients with centrally located tumours.

Moreover, risk-adaption of the total dose might also be advantageous. Especially for patients with severe comorbidity, Guckenberger (2015) argues that doses above approximately BED_{10}=105 Gy to the periphery of PTV, and approximately BED_{10}=170 Gy to central parts of the tumour, might not be beneficial. This implies that too high a dose might lead to severe side-effects for these patients, a conclusion depending on the dose to normal tissues which however was not reported.

3.3 Stereotactic coordinate system and immobilisation

A stereotactic frame with a coordinate system for robust immobilisation was a prerequisite for the high geometrical accuracy during the time period when routine online image-guidance was not available. The frame together with a soft-tissue image verification procedure made it possible to achieve the accuracy required for delivery of stereotactic treatments.

With the stereotactic body frame (SBF), the patient was positioned is a custom fitted vacuum pillow placed in a frame with a stereotactic coordinate system (Figure 5 left). This stereotactic coordinate system was visible on the CT images which allowed the tumour position to be located in the stereotactic system at treatment planning, as well as accurate patient positioning and tumour localisation at treatment. To improve the reproducibility of positioning the patient in the SBF, skin tattoos at sternum and tibia were applied and used for adjustment via laser systems attached to the frame; later the tattoos at the tibia were omitted. For patients with large breathing motions, an abdominal compression plate was placed on the patients' upper abdomen to reduce breathing motions (Figure 5 right). The breathing motion was initially assessed with fluoroscopy, and in later years with four-dimensional CT (4DCT).

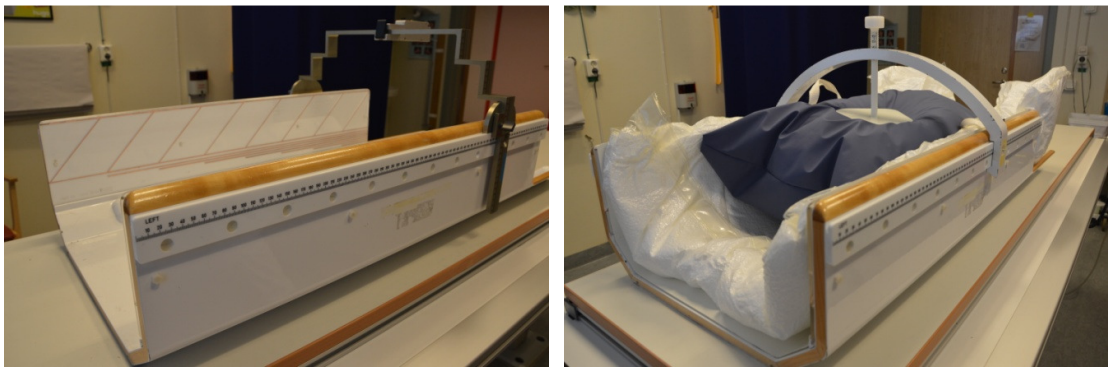

Figure 5*: The stereotactic body frame with the external coordinate system (left), and possibility for abdominal compression (right).*

With the introduction of online image-guidance, several other immobilisation systems have been developed for SBRT. Some of them employ a more or less frameless manner and only a few are available with a stereotactic coordinate system. Frequently these systems consist of a custom fitted vacuum pillow. Some clinics use devices, such as infrared markers placed on the patient's chest, to monitor patient motions during treatment (Jin *et al*., 2007). In a comparison of different immobilisation system devices, the SBF had the highest reproducibility (Shah *et al*., 2013). Besides the abdominal compression, breathing motions may be handled with gating and tracking techniques (Verellen *et al*., 2007; Verellen *et al*., 2010).

3.4 Heterogeneous dose distribution

Both intracranial SRT and SBRT deal with treatment of gross tumours. Thus increasing the dose inside the GTV as compared to the peripheral dose, with a heterogeneous dose

distribution, is likely to be advantageous. Especially considering the potentially more hypoxic and radioresistant cells within the GTV, even though the hypoxic cells might not be located exclusively in the central part of the tumour (Kavanagh & Cardinale, 2005). However, with a beam geometry approaching a 4π geometry, *i.e.* with the usage of non-coplanar beams, the dose increase to the central parts of GTV may be obtained without substantially increasing the dose to normal tissues outside the GTV (Lax, 1993). Thus, there is no price to pay for the "extra dose" to central volumes of the tumour that may contain more radioresistant cells.

Before the advent of optimisation algorithms for treatment planning systems, heterogeneous dose distribution was generated with field sizes smaller than the PTV (Lax, 1993). Today, the concept of heterogeneous dose distributions in SBRT is generally adopted, with the degree of dose distribution heterogeneity varying between different treatment centres and techniques. Prescription isodoses, at the periphery of the PTV, commonly range from the 65% to 90% isodose line, with heterogeneities up to a 50% higher dose within the GTV compared to the periphery of PTV. At the Karolinska University Hospital prescription is typically to the 67% isodose encompassing the PTV. There is still no consensus or guidelines on how to report doses in SBRT, and the variation in dose heterogeneity can complicate the comparison of the true biologic effect for the same prescription dose between different treatment centres (Kavanagh & Cardinale, 2005).

3.5 Tumour position verification

Today, to obtain a high geometrical accuracy of the treatment, online soft-tissue (or implanted marker) image-guidance is generally used in the setup process in SBRT. However, at the beginning of SBRT in the early 1990s, imaging in the treatment room was limited to planar MV-images on x-ray films. Thus, image verification of the tumour position in the stereotactic coordinate system was done with a verification CT, taken in free-breathing as in the treatment-planning CT, before the first treatment fraction was given (Lax, Blomgren, Larson, & Näslund, 1998). If the tumour was localised outside the PTV in the verification CT as compared to the treatment-planning CT, the stereotactic coordinates were adjusted. Since the verification of the tumour position was not done exactly at the time of treatment, the verification CT provided a probabilistic verification of the tumour position reproducibility (Lax & Blomgren, 2005). Today, with improved image-guided radiation therapy (IGRT), the tumour position is verified online with CBCT with the patient in the treatment position in the treatment room before the delivery of each treatment fraction. The CBCT scan is acquired over a period of several breathing cycles, giving a blurred image of moving structures. Other imaging systems for tumour position verification used today are, for example, ultrasound (Benedict, 2005), orthogonal kV-images and 4D-CBCT. With 4D-CBCT, both target visibility and localisation are improved in the presence of breathing, and the inter-observer target localisation variability is reduced, compared to 3D-CBCT (Sweeney *et al.*, 2012).

3.6 CTV-to-PTV margins and breathing motion assessment

At the start of SBRT at the Karolinska University Hospital, a verification CT was made before delivery of each fraction. In that way, data were collected to determine standard CTV-to-PTV margins. These were determined to be, and have so been since that time, 10 mm in the longitudinal direction and 5 mm in the transversal direction, if the assessed breathing motion was within 10 mm in the longitudinal direction and 5 mm in the transversal direction. This margin was estimated to have sufficient dose coverage of the tumour in 95% of the treatments (Lax & Blomgren, 2005; Lax *et al.*, 1998). If the tumour breathing motion, evaluated before the treatment planning, exceeded these limits, abdominal compression was applied which commonly reduced the breathing motions. If the tumour breathing motion still exceeded 10 mm in the longitudinal direction or 5 mm in the transversal direction, or if the abdominal compression did not reduce the motion, the CTV-to-PTV margin was increased to the same magnitude as the breathing motion amplitude, evaluated in each direction.

The breathing motion was at the beginning assessed with fluoroscopy of the diaphragm as a surrogate for the tumour, but subsequently, the tumour was assessed if visible. At the start, the motion was assessed in a frontal projection only. During that time, for small tumours located free in the lung parenchyma, a CTV-to-PTV margin of 10 mm was added isotropically around the CTV, due to the higher probability of baseline shifts for these tumours. In 2011 the assessment of tumour breathing motion was changed to 4DCT gated according to the patient's breathing. Both these methods of assessing the breathing motion are associated with certain limitations. When assessing the tumour motion only in a frontal projection there is a risk of underestimating the tumour motion in the anterior-posterior direction. A limitation with assessing the tumour motion with 4DCT is given by the short scan time over the tumour region, potentially underestimating the tumour motion, since the motion amplitude might vary between breathing cycles.

With the introduction of CBCT image-guidance, the setup accuracy was increased. For this reason, the CTV-to-PTV margins could in principle be decreased. This has not yet been done at the Karolinska University Hospital since it has not been known to what magnitude the margins could be decreased without reducing the probability of local tumour control. This was addressed in Paper IV where the results suggest that, averaged over the tumour population, the coverage probability for delivery of at least prescribed dose to 98% of CTV was improved from 90% to 99%, with the introduction of CBCT. That implies that the CTV-to-PTV margin could be decreased; this would be especially important if dose constraints to OAR are exceeded with standard margins. If the latter is not at risk, a disadvantage is that the local control of the tumour may be jeopardised with reduced margins. However, today there is still a lack of conclusive data as to whether a change from 90% coverage probability compared to 99% is reflected in the clinical outcome.

4 Clinical aspects of SBRT of lung tumours

Clinical outcome after radiotherapy is commonly evaluated with regard to local control (LC), local progression and toxicity, but might also be evaluated as overall survival (OS), cancer-specific survival, or local, regional or distant progression-free survival. In this chapter, local control and toxicity rates after SBRT of lung tumours, as well as in the specific case of reirradiation with SBRT after previous radiotherapy treatment, are reviewed.

4.1 Local control

The primary aim of radiotherapy is to achieve control of the irradiated tumour. The tumour response can be classified according to the Response Evaluation Criteria In Solid Tumours (RECIST) guidelines as complete response (CR) with total tumour disappearance, partial response (PR) with at least 30% tumour diameter-sum shrinkage, progressive disease (PD) with at least 20% tumour diameter-sum increase, or stable disease (SD) with no sufficient shrinkage (not PR) or increase (not PD) of the tumour diameter (Eisenhauer *et al*., 2009; Therasse *et al*., 2000).

The definition of local control might vary between including CR, PR and SD, or only CR and PR, but also freedom from PD. In published studies the local tumour effect is described by measures such as LC, local recurrence or relapse (LR), freedom from local recurrence (FFLR) or local progression (FFLP), cumulative local progression free rate and rate of CR, PR and SD, during the total follow-up time or at different time-points after treatment. There are numerous publications regarding tumour control after SBRT of lung tumours. The purpose of this review is not to evaluate the data quantitatively in detail but instead to illustrate the spread in published data of LC, or similar, for a relatively homogeneous group of lung tumours, mainly Stage I NSCLC. A summary of some published data on local tumour control or absence from local failure (FFLR, FFLP) versus prescribed dose in BED_{10}, regardless of the dose prescription point, is shown in Figure 6. The following sections provide some further elaborations on the relationship between dose and local tumour effect in SBRT of lung tumours.

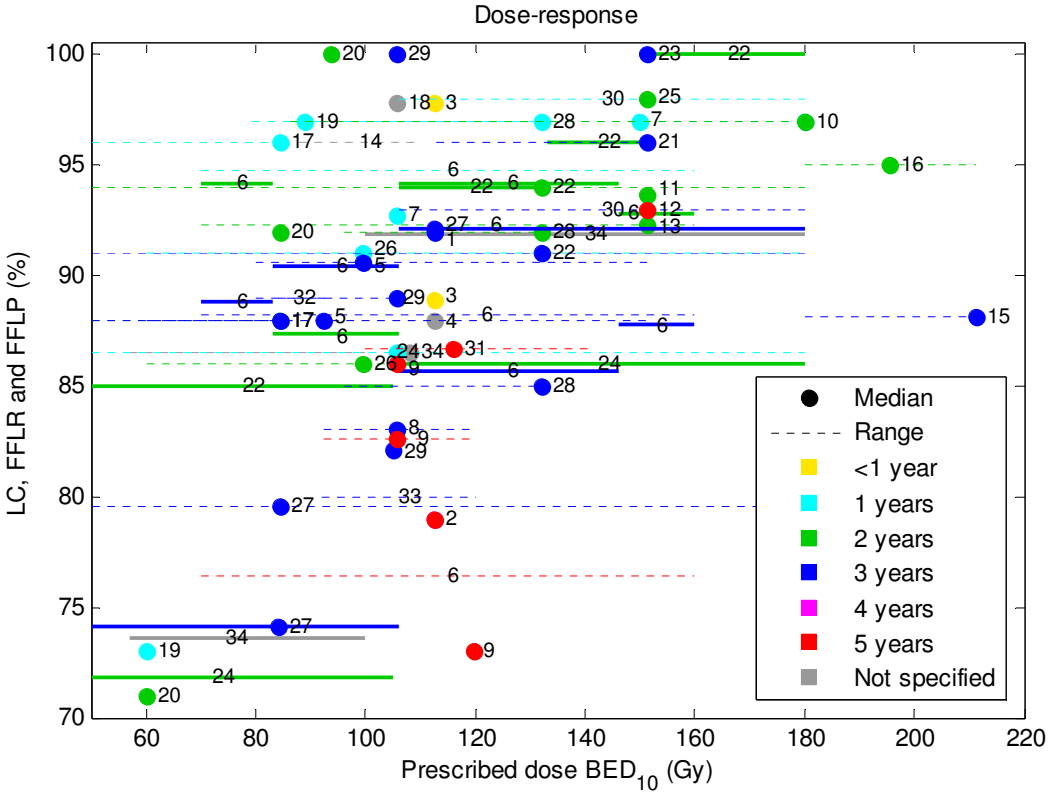

***Figure 6**: Published data on local control (LC) and freedom from local recurrence (FFLR) or local progression (FFLP), at different prescribed doses (regardless of the prescription point, but most commonly to the PTV periphery), and different time-points. Data points with LC below 70% have been omitted in the figure; these were LC at 3 years from reference 28: 44% at median BED_{10}=105.6 Gy (range 39-180 Gy), reference 32: 57% at BED_{10}=84 Gy (4 Gy × 15), and reference 35: 63% at BED_{10}<80 Gy. Thicker lines indicate references presenting data at several dose levels.*

Corresponding references to the numbers in the figure:

Nordic SBRT study group
1. Baumann *et al.* (2009)
2. Lindberg, Nyman, *et al.* (2015)
3. Nyman, Johansson, and Hultén (2006)
4. Baumann *et al.* (2006)

Meta-analyses
5. van Baardwijk *et al.* (2012)
6. Zhang *et al.* (2011)

Prospective studies
7. Videtic *et al.* (2015)
8. Shibamoto *et al.* (2012)
9. Shibamoto *et al.* (2015)
10. van der Voort van Zyp *et al.* (2010)
11. Timmerman *et al.* (2009)
12. Timmerman, Hu, *et al.* (2014)
13. Timmerman *et al.* (2013)
14. Grills *et al.* (2010)
15. Fakiris *et al.* (2009)
16. Timmerman *et al.* (2006)
17. Zimmermann *et al.* (2006)
18. Nagata *et al.* (2005)
19. Wulf *et al.* (2004)
20. Wulf, Baier, Mueller, and Flentje (2005)

Pooled cohort studies
21. Chang *et al.* (2015)
22. Grills *et al.* (2012)

Retrospective studies
23. Shaverdian *et al.* (2016)
24. Chik, Cheung, Lam, Kwan, and Au (2015)
25. Peulen, Belderbos, Rossi, and Sonke (2014)
26. Boda-Heggemann *et al.* (2014)
27. Guckenberger, Allgäuer, *et al.* (2013)
28. Baschnagel *et al.* (2013)
29. Shirata *et al.* (2012)
30. Lagerwaard *et al.* (2012)
31. Onishi *et al.* (2011)
32. Guckenberger *et al.* (2009)
33. Baba *et al.* (2009)
34. Onishi *et al.* (2004)

There are both proponents (Grills *et al*., 2012; Videtic *et al*., 2015) and opponents (van Baardwijk *et al*., 2012; Zhang *et al*., 2011) of the statement that there is a dose-response relationship within the high dose region above about BED_{10}=105 Gy or local control above about 85%. However, there seems to be a consensus that a certain minimum dose has to be given in order to get local control above 90% (Boda-Heggemann *et al*., 2014; Chik *et al*., 2015; Grills *et al*., 2012; Guckenberger, Allgäuer, *et al*., 2013; Guckenberger *et al*., 2009; Kestin *et al*., 2014; Onishi *et al*., 2004; Senthi, Haasbeek, Slotman, & Senan, 2013; Shirata *et al*., 2012; Wulf *et al*., 2005). A phase II clinical trial in the Nordic countries, including Karolinska, of SBRT of NSCLC showed a LC of 92% at 3 years (Baumann *et al*., 2009). The long-term follow-up of these patients showed a local control of 79% at 4 and 5 years (Lindberg, Nyman, *et al*., 2015). In this trial 15 Gy × 3 (BED_{10} = 113 Gy) was prescribed to the periphery of PTV, corresponding to approximately the 67% isodose, and it was conducted before online image-guidance was available.

The dose reported in SBRT is most often the prescribed dose which generally is at the periphery of the PTV. However, in some cases, the dose is prescribed to the isocenter, located centrally in the CTV. There is an ambiguity in published data whether the periphery dose to the tumour or the central dose correlates to the probability of local control. Guckenberger, Klement, *et al*. (2013) imply that generally there is a better correlation between local tumour control and the maximum PTV dose than with the PTV periphery dose. In addition, van Baardwijk *et al*. (2012) concluded that there is no significant relationship between freedom from local progression and the dose to the periphery of PTV, from a meta-analysis of SBRT and accelerated high-dose conventional RT for NSCLC. However, Wulf *et al*. (2005) concluded from multivariate analysis (including isocenter dose, PTV periphery dose, tumour size and primary tumour or metastasis) that the dose to the PTV periphery was the only significant parameter for local control. A complicating factor to this question is that there have been different degrees of heterogeneity of the dose within the PTV in different studies.

The different conclusions reached in the studies mentioned above may also be due to the differences between the reported prescribed or planned dose and the actually delivered dose. In Paper IV a lower delivered dose to the CTV was estimated using image-guidance with pre-treatment verification CT, compared to using online CBCT image-guidance. However, the increase in delivered dose to the CTV periphery with the methodological change from pre-treatment verification CT to online CBCT image-guidance does not seem to be reflected in available data of local control. Baumann *et al*. (2009) presented a local control of 92% after 3 years with the use of pre-treatment verification CT, while studies using online image-guidance do not seem to present higher figures of local control, however, with a variety of prescribed doses (Baschnagel *et al*., 2013; Boda-Heggemann *et al*., 2014; Grills *et al*., 2012; Nyman *et al*., 2016). Moreover, different CTV-to-PTV margins may have been used in the literature, leading to different levels of spatial accuracy; this could also influence the expected local control.

To demonstrate a significant increase in LC from about 90% to a hypothesised figure of 95% at a higher tumour dose, the required patient-cohort size would depend on the unknown gradient from the 90% to 95% LC in the corresponding dose-response curve. Clinical data after more than 15 years of worldwide use of SBRT does not seem to provide an answer to the question of this dose response. If there is a high clinical demand for local control above 95%, rather than of the order of 90%, good estimates of delivered dose rather than prescribed doses will probably be highly important for the future to solve the issue of dose response.

Besides the prescribed dose and the delivered dose, there might be technical-, patient- or tumour-related factors influencing the risk of local recurrence, such as:

- Uncertainties in tumour delineation, depending on the diagnostic tools, image quality, image modality and experience of the operator. Baumann *et al.* (2006) discuss whether an observed increase in local failures for centrally located tumours was caused by the difficulty to distinguish between mediastinal structures and tumour growth, but it might also have been due to planned underdosage of the PTV or even the CTV due to proximity to OAR, or breathing motion.
- Tumour size (number of clonogenic cells). There are reports of larger tumours being a risk factor for local recurrence (Baumann *et al.*, 2006; Peulen *et al.*, 2014; Zhao *et al.*, 2015), even though Allibhai *et al.* (2013) conclude from a prospective risk-adapted study that tumour size is not correlated with local failure, but with overall survival.
- Radioresistant hypoxic cells, or cells in a radioresistant phase of the cell cycle, which require a dose that is 2.5-3 times higher than the dose needed for non-hypoxic cells in a more radiosensitive phase (Fowler *et al.*, 2005). The heterogeneous dose distribution, with up to 50% higher doses in the central parts of the tumour compared to the prescribed dose to the periphery of PTV, might therefore not be enough for local control.
- Patient- or tumour-individual radiosensitivity depending on genetic factors or histological tumour type, which has been shown in cell studies (Malaise, Fertil, Chavaudra, & Guichard, 1986; Skiöld *et al.*, 2015; Williams *et al.*, 2008).

The ultimate purpose of local control after SBRT is that of cure or improved survival or improved well-being of the patient. But, even if local tumour control is achieved, cure or overall survival might not be improved (Boda-Heggemann *et al.*, 2014; Guckenberger, 2015). This non-intuitive result might be caused by distant metastases, comorbidity and high patient age. In contrast to studies showing that, others have shown improved survival with high-dose SBRT (Baumann *et al.*, 2006; Guckenberger, Allgäuer, *et al.*, 2013; Palma *et al.*, 2010). However, Zhang *et al.* (2011) observed lower OS at 2 and 3 years for patients treated with BED_{10}>146 Gy compared to those treated with BED_{10}=83-146 Gy in a meta-analysis. The authors mention that this may be due to increased toxicity, but argue that such a conclusion should be interpreted with caution due to potential differences between the included studies.

4.2 Toxicity

4.2.1 Radiation-induced damage

If further increase of dose is not the decisive factor for improving the local control, then it might be more relevant to limit the incidence of toxicity, as radiation-induced toxicity can have a substantial effect on the quality of life and can even be life-threatening or lead to death. The severity of radiation-induced damage depends on the radiation dose delivered to different tissues or organs, the volume irradiated, fractionation schedule, concomitant treatment, and additionally patient-specific aspects such as general health, comorbidity and genetic factors (such as radiosensitivity) (Steel, 2007). To prevent or limit serious toxicity, the treatment plan is designed to limit the dose to sensitive OAR. There are different kinds of dose constraints for different OAR, such as maximum dose, mean dose or dose-volume constraints, depending on the specific side-effects, based on clinical studies and clinical experience.

Which kind of dose constraints that should be applied to the different organs depends on dose-response data for each specific end-point. If there is a small volume effect associated with the dose response the organ is classified as *serial*. With a large volume effect it is classified as *parallel*. The terms serial and parallel refers to the structural organisation of functional subunits (FSUs) assumed in the model describing the dose response. Serial organs can be thought of as a chain of FSUs that all have to be preserved to keep the functionality of the organ, and are sensitive to maximum point doses or close to the maximum dose (ICRU, 2010). Parallel organs have FSUs that act independently of each other (ICRU, 2010), so that a certain volume (threshold volume) can be destroyed (due to being irradiated to a threshold dose) without the organ losing the function, owing to its functional reserve (Timmerman & Lohr, 2005). If a part of a parallel organ, like peripheral lung or peripheral liver, is damaged due to a too high dose, other parts of the organ can compensate for the loss of function, providing the damaged part does not exceed a critical volume. Parallel tissues are not sensitive to high-dose points, but rather the mean dose, or the irradiated volume at a certain dose level, *i.e.* if a threshold volume has been destroyed (ICRU, 2010). The lungs can be considered as a combination of the two structure types, with the serial structure of the trachea and bronchi, and parallel structure of the alveoli-capillary complexes in the lung parenchyma (Timmerman & Lohr, 2005).

To be able to compare toxicity data between treatment centers, the evaluation of side-effects needs to be consistent. However, there are different toxicity scales available, with similarities and differences. One of the most commonly used is Common Terminology Criteria for Adverse Events (CTCAE) (National Cancer Institute, 2010), with a grading from one (with none or mild symptoms) to five (with side-effects leading to death) (see Table 2).

***Table 2**: General summary of toxicity grading according to CTCAE version 4.0.*

Toxicity grade	Symptoms
Grade 1	Asymptomatic or mild symptoms, no intervention required
Grade 2	Moderate symptoms, or limited instrumental ADL, or medical or non-invasive intervention
Grade 3	Severe symptoms, or limited self-care ADL, or hospitalisation, or operative intervention
Grade 4	Life-threatening, or urgent intervention
Grade 5	Death

ADL = activities of daily living (instrumental ADL is cooking, shopping, handle private economy, etc; self-care ADL is dressing, personal hygiene, etc (National Cancer Institute, 2010))

Irradiation of lung tumours can induce toxicity due to damage to different structures in the lungs or nearby, such as the trachea, bronchi, alveoli, blood vessels, chest wall, heart, esophagus and spinal cord. It is recommended that circumferential irradiation of tubular organs is avoided of any critical structures (Grimm *et al*., 2011; Videtic *et al*., 2014). Depending on the tumour extent and location relative to OAR, the probability of different side effects varies. The incidence and severity of toxicity are related to higher doses (Zhang *et al*., 2011), and to central or peripheral tumour location (Bral *et al*., 2011).

4.2.2 Timeframe of toxicity

The time for the manifestation of radiation response varies between different kinds of cells, due to diversity in lengths of cell cycles. The timeframe might range from a few hours to several years. Toxicity is often classified into acute or early toxicity and late toxicity. Early toxicity is generally defined as that appearing within 3 months from radiotherapy, while late toxicity appears after 3 months up to several years after the treatment. The early-responding cells are those that proliferate fast, like epithelial cells, and respond to radiation within weeks from treatment (Steel, 2007). A short overall treatment time will reduce the cell repopulation time, which is an extra burden on healthy cells but an advantage in terms of tumour control (Steel & Nahum, 2007). Late-responding cells, like in the lungs and spinal cord, have a slower proliferation and express damage after weeks or years after the treatment (Steel, 2007). These cells are less affected by the overall treatment time (Steel & Nahum, 2007). Late-responding cells are more sensitive to the dose per fraction than early-responding cells (Steel & Nahum, 2007). Early side-effects are often temporary and heal, while late side-effects might be chronic (Dobbs & Landberg, 2003; Steel, 2007).

4.2.3 Toxicity after SBRT of centrally located lung tumours

Especially for centrally, compared to peripherally, located lung tumours, severe toxicity and death after SBRT have been observed (Haseltine *et al*., 2016; Timmerman *et al*., 2006). For these tumours, the distance to radiosensitive OAR generally decreases, leading to increased probability of high doses to OAR which may cause toxicity. From a systematic review by Senthi *et al*. (2013) of 20 studies including 563 centrally located primary NSCLC tumours or lung metastases treated with SBRT, the risk of grade 3-4 toxicity is reported to be less than 9%, which might still be higher compared to patients treated for peripheral tumours. This is supported by Fakiris *et al*. (2009) who observed a rate of grade 3-5 toxicity of 10% for

patients with peripheral tumours, and 27% for those with central tumours. Furthermore, Timmerman *et al*. (2006) concluded from a phase II study of SBRT-treated NSCLC that there is an 11-fold higher risk of severe side-effects for patients with centrally located tumours (within 2 cm from the proximal bronchial tree) compared to patients with peripherally located tumours. Bezjak *et al*. (2016) report a maximum tolerated dose of 12 Gy × 5 from a dose-escalation phase I/II study (RTOG 0813) of SBRT for centrally located NSCLC (within 2 cm from the proximal bronchial tree, or close to mediastinal or pericardial pleura), with 7% dose-limiting toxicity at this dose level. However, Chaudhuri *et al*. (2015) treated central tumours abutting the bronchi with 10 Gy × 5 or 12.5 Gy × 4, and did not observe any grade 2 or higher toxicity. Due to the proximity to OAR for centrally located lung tumours, a prolonged treatment schedule with more number of fractions might be advantageous (Guckenberger, 2015; Timmerman & Lohr, 2005), but might be at the expense of decreased tumour control (Timmerman & Lohr, 2005).

4.2.4 Toxicity related to organs in the vicinity of the lungs

Toxicity related to the organs in the vicinity of the lungs are fatigue, pleural effusion, chest wall pain and rib fractures, skin necrosis, esophagitis, pericardial effusion, brachial plexopathy and spinal cord damage.

- **Fatigue** is a general weakness with inability to perform daily activities (National Cancer Institute, 2010).
- **Pleural effusion** is the collection of fluid in the pleural cavity surrounding the lungs (National Cancer Institute, 2010). This fluid is usually reabsorbed after some months without any intervention (Timmerman & Lohr, 2005).
- **Chest wall pain and rib fractures**. Chest wall pain seems especially to be a problem for patients with tumours in the dorsal part of the lungs, close to the spine, with irradiation of the roots of the chest wall nerves. Rib fractures might be subclinical, *i.e.* without symptoms (Baumann *et al*., 2006).
- **Skin necrosis**. Irradiation with high dose in the skin may trigger a necrotic process. For calculation of skin dose, the skin is commonly defined as a 5 mm thick layer from the body surface (Grimm *et al*., 2012).
- **Esophagitis** is an inflammation of the esophageal wall, while esophageal stenosis or perforation is narrowing or rupture of the esophageal lumen (National Cancer Institute, 2010). Perforation of the esophagus requires food intake through percutaneous endoscopic gastrostomy, which might have a large impact of quality of life, and can also be life-threatening.
- **Pericardial effusion** is the collection of fluid in the sac surrounding the heart (National Cancer Institute, 2010), which can cause pressure on the heart and thereby reduced heart function. Further, long-term effects of lethal damage to the heart tissue can be caused by radiation. The coronary vessels seem to be the most radiosensitive parts of the heart, where high doses might disrupt the electrical impulses for the heart beat.

- **Brachial plexopathy** is a destruction of the nerves to the arm and hand on the affected side. The brachial plexopathy can cause numbness, tingles, pain, weakness, and reduced function of the arm or hand (National Cancer Institute, 2010). Risk factors include large tumours located in the apex of the lungs and the maximum dose to the brachial plexus (Lindberg, Grozman, *et al*., 2015).
- **Spinal cord damage**. Myelitis is inflammation of the spinal cord which might lead to tingle, weakness and sensory loss (National Cancer Institute, 2010). Spinal cord damage can lead to paralysis (myelopathy) of the body (Steel, 2007), from the damaged point and downwards. Since this is a very serious toxicity, it is highly prioritised to be avoided despite potentially limiting the probability of tumour control.

4.2.5 Toxicity related to the lungs

Different kinds of toxicity related to the lungs are cough, dyspnea, fibrosis, pneumonitis, pneumonia, haemoptysis and atelectasis.

- **Cough** may appear with mild coughing up to severe coughing limiting the self-care activities of daily living (ADL) (National Cancer Institute, 2010).
- **Dyspnea** is difficulty in breathing (National Cancer Institute, 2010), with shortness of breath or breathlessness. This is common after radiotherapy treatment with fibrosis in the lungs, leading to limitations in expanding the lungs at inhale and retracting at exhale. Many patients with lung cancer are smokers with COPD, with breathing difficulties due to enlarged alveoli and lungs with limited breathing dynamics, already prior to the cancer treatment.
- **Fibrosis** is a reaction to radiotherapy, in which the lung tissue is replaced by connective tissue (National Cancer Institute, 2010). The lung parenchyma loses its elasticity, with thickening around the small bronchi and blood vessels, and reduced ability to oxygen exchange (Timmerman & Lohr, 2005). This might appear a year or more after irradiation (Steel, 2007).
- **Pneumonitis** is a radiation-induced sterile lung inflammation of the lung parenchyma. Symptoms might be fever, dry cough, chest pain and dyspnea (Timmerman & Lohr, 2005). This decreases the patient's breathing capacity, since the ability for the air to come into the alveoli and the oxygen-carbon dioxide exchange is reduced (Timmerman & Lohr, 2005). This side effect generally appears 3-6 months after radiotherapy (Steel, 2007).
- **Pneumonia** is a bacterial (or sometimes viral) infection causing lung inflammation with symptoms like fever, cough and respiratory distress, and is commonly treated with antibiotics. Fatal pneumonia has been reported after SBRT of both central and peripheral tumour locations (Timmerman *et al*., 2006).
- **Haemoptysis** is coughing up blood or blood-stained mucus from the airways. Haseltine *et al*. report about 4 out of 18 (22%) patients with treatment-related death, of which 2 were due to pulmonary hemorrhage, after SBRT of tumours touching the proximal bronchial tree (Haseltine *et al*., 2016). The cause of bleeding after treatment

of centrally located lung tumours is not known in detail. One reason might be high doses to the bronchi or to vessels in the bronchial wall. Another reason might be that the tumour grows into the bronchial wall, not related to the treatment but to disease progression.

- **Atelectasis** is the collapse of the lung parenchyma, either limited to a segment of the lung, or a lung lobe, or extending to a whole lung (National Cancer Institute, 2010). This side effect might be asymptomatic, diagnosed on radiological findings, if the collapsed volume is less than the patient's lung reserve (Timmerman & Lohr, 2005), or might have a major impact on the patient's breathing. Baumann *et al*. observed atelectasis for patients with centrally located lung tumours or tumours close to the main bronchi (Baumann *et al*., 2006). Whether the cause of atelectasis is bronchial damage with obstruction of the airway, vascular damage with blocked supply of blood, or a combination of these, is not known (Timmerman & Lohr, 2005). Furthermore, whether the effect of irradiating the whole cross-section of a bronchus is more pronounced or not in terms of incidence of atelectasis, compared to only irradiating a part of the bronchial wall with a certain dose level, is also not known.

Due to the observed atelectases by Baumann *et al*. (2006), we conducted a retrospective study of radiation-induced atelectasis (Paper II) which shows that there is a correlation between the maximum dose to the bronchi and radiation-induced atelectasis (Karlsson *et al*., 2013). Among the 64 patients with available dose-volume data for the bronchi, 49 patients (77%) did not show signs of atelectasis and 15 patients (23%) developed atelectasis considered to be radiation induced, during the median follow-up period of 12 months (1-82 months). The median of the minimum dose to 0.1 cm^3 of the bronchi receiving the highest dose ($D_{0.1cm3}$) was EQD_2=105 Gy_3 (mean 124 Gy_3, range 20-279 Gy_3) for the patients who did not develop atelectasis, and 210 Gy_3 (mean 213 Gy_3, range 98-293 Gy_3) for the patients who did. The incidence of atelectasis at different intervals of bronchial doses can be seen in Figure 7, without consideration of different follow-up times, together with the estimated dose-response relationships at 1, 2 and 3 years after treatment, however, with wide confidence intervals. The atelectases were developed at a median time of 8 months (mean 10 months, range 1-30 months) after treatment. Kaplan-Meier curves for time to atelectasis are shown in Figure 8, with a significant difference for patients with bronchial $D_{0.1cm3}$ above or below the median dose 147 Gy_3 (log-rank $p<0.001$).

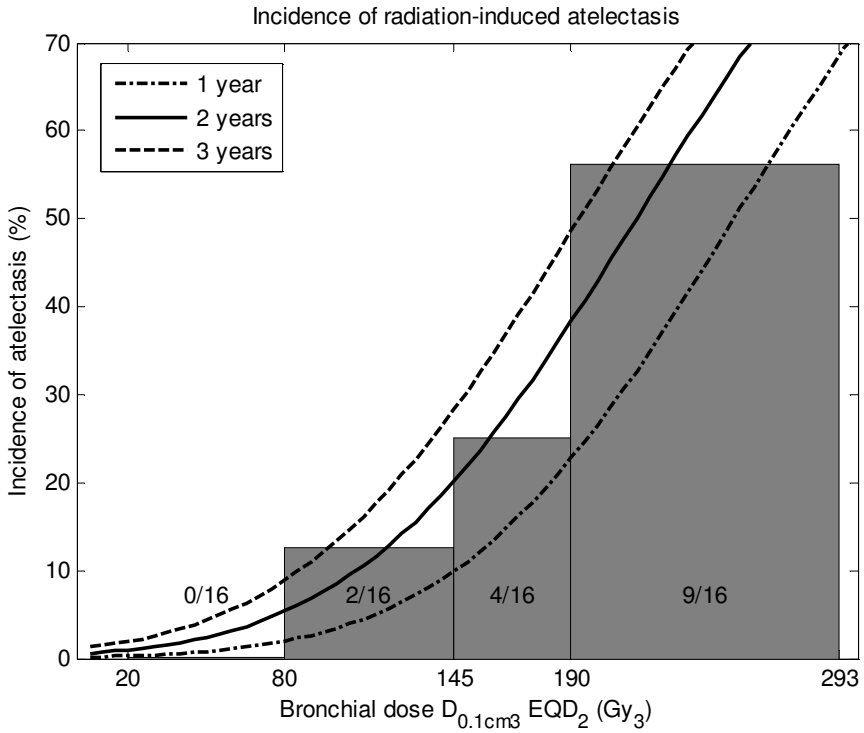

***Figure 7**: Incidence of radiation-induced atelectasis (number of patients with atelectasis divided by the number of patients in total) at different intervals of bronchial doses ($D_{0.1cm3}$) in EQD_2, not considering different follow-up times for the patients. The superimposed curves are estimated dose-response relationships at different times after treatment.*

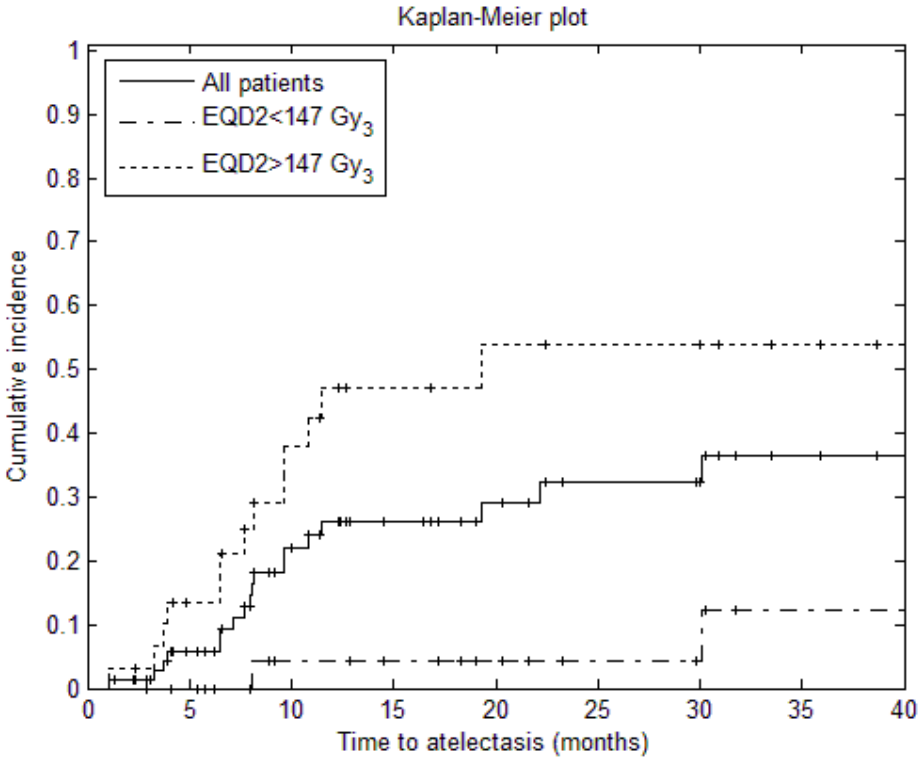

***Figure 8**: Cumulative incidence of atelectasis with time, for all patients (solid line) and for those receiving a bronchial dose $D_{0.1cm3}$ of EQD_2<147 Gy_3 (dash-dotted line) and EQD_2>147 Gy_3 (dotted line), markers (+) indicate censored patients.*

As a comparison, Duijm *et al*. presented atelectasis incidence for the lobar and segmental bronchi, in a study of 104 evaluated patients with centrally located tumours treated with SBRT (Duijm, Schillemans, Aerts, Heijmen, & Nuyttens, 2016). The lobar bronchi received a median maximum dose (D_{max}) of EQD_2=124 Gy_3 (range 67-233 Gy_3); after 1 year 12% had developed atelectasis and after 2 years 19%, while the segmental bronchi received a median D_{max} of EQD_2=121 Gy_3 (range 39-245 Gy_3); after 1 year 24% had developed atelectasis and after 2 years 30%. These results indicate that the segmental bronchi might be more sensitive to radiation than the lobar bronchi.

4.2.6 Toxicity and dose constraints

The most common target today for SBRT is lung tumours of a relatively limited volume, resulting in low toxicity. However, all toxicity end-points and organs at risk listed above, associated with SBRT, are of increasing importance due to the widening of indications for SBRT. Due to limitations in follow-up data for many toxicity end-points, dose-response relationships used in SBRT are uncertain and in many cases based on data from conventional RT. To what extent the predictive models from conventional RT are applicable to SBRT might be questioned (Timmerman & Lohr, 2005).

In the literature, dose data refer mainly to the prescribed or planned doses, which might deviate from the delivered dose that generated the outcome studied, such as local control, progression-free survival and toxicity. Even though this to some extent is a disadvantage since the predictive model (and in general the data analysis) is based on inaccurate doses, an advantage is that it corresponds to clinical practice when evaluating doses in a treatment plan before treatment, since only the *planned* dose can be evaluated at that stage. The importance in that case is that the systematic uncertainties between planned and delivered dose are the same for the evaluated patient as for the patients that contributed to the predictive model. This requires that the same treatment methodology was used for the modelled patients as for the evaluated patient.

In Table 3 literature data on dose constraints for a few selected kinds of toxicity relevant for SBRT of central lung tumours are listed. The data refer to constraints selected in clinical trials (RTOG and LungTech) and from the follow-up. The purpose of the table is to illustrate the spread in dose-volume constraints used, reflecting the lack of solid data for relevant levels of constraints. The reason for lack of accurate dose constraints is primarily due to a limited amount of relevant follow-up data, further complicated by the possible differences between the planned dose to OAR and the delivered one. This is expected to be a more pronounced factor in SBRT compared to conventional radiotherapy due to the steeper dose gradients in SBRT.

***Table 3**: Data on selected dose constraints relevant for centrally located lung tumours and reported outcome of different kinds of toxicity.*

Toxicity	Reference	Study type	No of pts.	No of fract.	Dose constraints (Gy)	EQD_2 constraints (Gy_3) *	Endpoint	Toxicity
Trachea and main bronchus								
Trachea and main bronchus **	RTOG 0915	Prospective	39	1	D_{max}< 20.2 , $D_{4\ cm3}$< 10.5	D_{max}< 93.7 Gy, $D_{4\ cm3}$< 28.4	Stenosis/fistula G≥3	None reported
Trachea and ipsilateral bronchus	RTOG 0618	Prospective	26	3	D_{max}< 30	D_{max}< 78		4 (16%) G3 tox not specified, no G4-5 tox
Trachea and main bronchus **	RTOG 0915	Prospective	45	4	D_{max}< 34.8, $D_{4\ cm3}$< 15.6	D_{max}< 81.4, $D_{4\ cm3}$< 21.5	Stenosis/fistula G≥3	None reported
Trachea and ipsilateral bronchus, non-adjacent wall	RTOG 0813	Prospective	120	5	D_{max}< 53-63, $D_{4\ cm3}$< 18	D_{max}<142-197, $D_{4\ cm3}$< 24	Stenosis/fistula	Unspecified tox: 9 G3, 1 G4, 1 G5
Trachea and main bronchus	LungTech 2015	Prospective		8	D_{max}< 44	D_{max}< 75		
Esophagus								
Esophagus **	RTOG 0915	Prospective	39	1	D_{max}< 15.4, $D_{5\ cm3}$< 11.9	D_{max}< 56.7, $D_{5\ cm3}$< 35.5	Stenosis/fistula G≥3	None reported
Esophagus	RTOG 0618	Prospective	26	3	D_{max}< 27	D_{max}< 65		4 (16%) G3 tox not specified, no G4-5 tox
Esophagus **	RTOG 0915	Prospective	45	4	D_{max}< 30, $D_{5\ cm3}$< 18.8	D_{max}< 63, $D_{5\ cm3}$< 29	Stenosis/fistula G≥3	None reported
Esophagus, non-adjacent wall	RTOG 0813	Prospective	120	5	D_{max}< 53-63, $D_{5\ cm3}$< 27.5	D_{max}< 142-197, $D_{5\ cm3}$< 46.8	Stenosis/fistula	Unspecified tox: 9 G3, 1 G4, 1 G5
Esophagus	LungTech 2015	Prospective		8	D_{max}< 40	D_{max}<64		
Heart								
Heart/pericardium	RTOG 0915	Prospective	39	1	D_{max}< 22, $D_{15\ cm3}$< 16	D_{max}< 110, $D_{15\ cm3}$< 61	Pericarditis G≥3	None reported
Heart/pericardium	RTOG 0618	Prospective	26	3	D_{max}< 30	D_{max}< 78		4 (16%) G3 tox not specified, no G4-5 tox
Heart/pericardium	RTOG 0915	Prospective	45	4	D_{max}< 34, $D_{15\ cm3}$< 28	D_{max}< 78, $D_{15\ cm3}$< 56	Pericarditis G≥3	None reported
Heart/pericardium	RTOG 0813	Prospective	120	5	D_{max}<53-63, $D_{15\ cm3}$< 32	D_{max}< 142-197, $D_{15\ cm3}$< 60	Pericarditis	1 G3 bradycardia (slow heart rate), unspecified tox: 9 G3, 1 G4, 1 G5
Heart	LungTech 2015	Prospective		8	No restriction	No restriction		

* Recalculated with the LQ model using α/β=3Gy, ** Avoid circumferential irradiation, G = grade, References: RTOG 0915 (Videtic *et al*., 2015; Videtic *et al*., 2014), RTOG 0618 (Timmerman, Pass, *et al*., 2014; Timmerman *et al*., 2013), RTOG 0813 (Bezjak *et al*., 2014; Bezjak *et al*., 2016), LungTech 2015 (Adebahr *et al*., 2015)

4.3 Reirradiation

Reirradiation of a previously irradiated volume may be needed due to local recurrence or new tumours (primary or metastases). There is an increasing need to know more about the applicability and limitations with reirradiation with SBRT. If the location of the second target is close to the previous one, careful considerations have to be taken to previously delivered doses to OAR. The risk of toxicity due to the accumulated dose is the limiting factor for re-treatment.

If a long time has passed since previous treatment, it might be possible to neglect some of the delivered dose due to recovery from previous damage, but the extent to which this is possible is not well known and varies between different kinds of organs and cells. According to a review by Mantel *et al*., early-responding tissues show almost complete repair within a few months, while recovery of late-responding tissues is more organ specific (Mantel, Flentje, & Guckenberger, 2013).

Times to local relapse of lung tumours after SBRT is reported to be between 3-76 months (Baumann *et al*., 2006; Grills *et al*., 2010; Guckenberger *et al*., 2009; Lagerwaard *et al*., 2012; Lindberg, Nyman, *et al*., 2015; Wulf *et al*., 2005). From Figure 6 it may be concluded that about 10% of lung tumours will develop local relapse. A new tumour on the other hand, close to a previous one, may appear at any time after the first.

Data on reirradiation of lung tumours in a previously irradiated region are scarce. Mantel *et al*. (2013) suggested in a review that SBRT should be used in order to fulfil the requirements of small treatment margins, relying on image-guidance, minimised intra-fractional uncertainties due to effective immobilisation and motion management, and highly conformal dose distributions, for a reduced risk of toxicity. Furthermore, the authors proposed that SBRT delivered with hypofractionated treatment schedules and shorter treatment time, compared to conventionally fractionated treatment, is advantageous since reirradiation often is delivered with palliative intent.

In Paper I, which was one of the first publications on reirradiation with SBRT, it was shown that this kind of reirradiation is feasible with the exception for centrally located tumours, where there is an increased risk of high-grade toxicity and mortality (Peulen *et al*., 2011). The prescribed dose to the periphery of the PTV at approximately the 67% isodose had a median of EQD_2=63 Gy_{10} (range 30-94 Gy_{10}) at the first treatment, and EQD_2=63 Gy_{10} (range 48-94 Gy_{10}) at the reirradiation. The median time between first treatment and reirradiation was 14 months (range 5-54 months), and the median follow-up time was 12 months (range 1-97 months). Out of the 29 patients studied, 3 deaths due to bleeding were observed, all with central tumour locations. It was not possible to assess any toxicity correlation with dose, since there were few events and with tumours located close to different OAR. No correlation between lung toxicity and mean lung dose (MLD) was found. The dose to larger vessels was inspected to investigate any correlation to the risk of bleeding, but no correlation could be

established. The local control rate 5 months after the reirradiation was 52%, and the overall survival at 1 and 2 years after the reirradiation was 59% and 43%, respectively.

Subsequently, others have published within the field. A study of SBRT as the first treatment with later reirradiation, or as the treatment used for reirradiation, was performed by Meijneke *et al*. (Meijneke, Petit, Wentzler, Hoogeman, & Nuyttens, 2013). Of the 20 patients included in their study, SBRT was the first treatment for 14 patients and conventional chemoradiotherapy was the first treatment for 6 patients. Meanwhile, reirradiation was done with SBRT for 18 patients, with curative conventional radiotherapy in 1 patient, and with palliative radiotherapy in 1 patient. The mean prescribed dose at the first treatment was EQD_2=133 Gy_{10} (range 44-150 Gy_{10}), and at reirradiation EQD_2=83 Gy_{10} (range 23-150 Gy_{10}), with the SBRT dose prescribed to the isodose line of 70-85% encompassing at least 95% of the PTV. The time from first treatment to reirradiation was in median 17 months (2-33 months). A summation of doses in EQD_2, with deformable registration, gave a median V_{20Gy3} to both lungs of 15% (range 3-47%), and a median MLD of 15 Gy_3 (range 4-28 Gy_3). There were 4 patients with MLD>20 Gy_3, 2 patients with V_{20Gy3} > 40%, 7 patients with ≥70 Gy_3 to the heart and the trachea, and 8 patients with ≥70 Gy_3 to the esophagus (range 71-123 Gy_3). No grade 3-5 toxicity was observed. The local control at 1 and 2 years was 75% and 50%, respectively, and the overall survival 1 and 2 years was 67% and 33%, respectively.

Patel *et al*. (2015) retrospectively reviewed 26 patients reirradiated with SBRT for 29 tumours, after previous conventional RT for 90% of the patients and SBRT for 10% of the patients, commonly in combination with chemotherapy. The median physical dose at first treatment was 61 Gy (range 30-74 Gy), and at reirradiation 30 Gy (range 15-50 Gy) in 3-5 fractions (reirradiation BED_{10} median 48 Gy, range 20-113 Gy) to the 69% isodose (range 55-85%). The median interval between treatments was 8 months (range 3-26 months). They did not observe any grade 3-5 toxicity. The LC rate at 1 and 2 years was 79% and 66%, respectively, and OS was 52% and 37%, respectively.

Hearn *et al*. have studied reirradiation using SBRT of local failures within 1 cm from a PTV previously treated with SBRT (Hearn, Videtic, Djemil, & Stephans, 2014). Of their 10 patients, 2 had tumours located close to the mediastinum, but not in the region of the proximal bronchial tree. The prescribed median dose at first treatment was BED_{10}=100 Gy (range 100-150 Gy), and BED_{10}=100 Gy (range 100-180 Gy) at the reirradiation, with a median time interval of 15 months (range 10-26 months). During a median follow-up time of 14 months (range 5-44 months) after reirradiation, 4 of the tumours had local progression, but no grade 3-5 toxicity was observed. They concluded that reirradiation with SBRT of BED_{10}≥100 Gy after previous SBRT is well tolerated for patients with peripheral tumours.

A consensus has therefore now been reached that reirradiation is a viable and effective treatment option, although tumour location should be carefully considered before selecting reirradiation therapy.

5 Geometric and dosimetric aspects of SBRT of lung tumours

Radiotherapy is primarily aiming at delivering a high dose to the tumour, and restricting the doses to OAR. This is a challenge, especially in SBRT, as prescribed doses are well above the dose-constraints of most OAR. This is the reason why SBRT is most commonly used in lung and liver tumours, since these organs have a functional reserve capacity and generally there is sufficient distance between the tumour and critical OAR. However, indications for SBRT are continuously pushed to more demanding cases with OAR located closer to the target. For this reason, as well as for accurate treatment delivery, geometrical uncertainties are very important to consider, and to a lesser extent also dosimetric uncertainties.

There are different ways of managing the geometrical and dosimetric uncertainties. The standard way is to, in the treatment planning, add safety margins around the tumour by constructing a PTV that includes all possible geometrical and dosimetric uncertainties in order to ensure delivery of prescribed dose to the whole CTV with an acceptable probability (ICRU, 1993, 1999, 2010). A newer approach is probabilistic treatment planning, where the uncertainties instead are accounted for during the optimisation process in the treatment planning.

5.1 Geometrical uncertainties

Geometrical uncertainties affecting the dose distribution depends on several factors such as breathing motion, tumour deformation and tissue changes, baseline shifts in tumour position, the breathing phase of the treatment-planning CT, structure delineation, patient positioning, image-guidance, machine geometry, and the human factor.

5.1.1 Breathing motion

The magnitude of breathing motion is generally larger in the longitudinal direction, and for tumours located close to the diaphragm. Evaluation of the breathing amplitude can be done through fluoroscopy or 4DCT. An evaluation of sinusoidal breathing motion amplitudes from different 4DCT systems in a lung phantom showed that the amplitude was underestimated, at a level of 82%-97% of the actual amplitude (1-4 cm), for a range of 4DCT systems (Nielsen, Hansen, Westberg, Hansen, & Brink, 2016).

Reduction of the breathing amplitude can generally be obtained with abdominal compression (Han *et al*., 2010; Karlsson, Gagliardi, Rutkowska, & Lax, 2008; Wunderink *et al*., 2008). However, for some patients the pressure changes the breathing pattern, from an abdominal to a more thoracic one, and sometimes with increased amplitude. Alternative techniques of managing breathing motion in RT are tracking, gating and breath hold.

Real-time **respiratory tumour/marker tracking** consists of online synchronisation of the treatment machine or the MLC and the tumour motion (Verellen *et al*., 2007). The tracking approach requires an accurate prediction model of the breathing motion. The breathing

pattern is usually obtained from an external signal, and a correlation model has to be established between this signal and the internal tumour motion. For the CyberKnife system, the tracking accuracy of lung tumours is better than 2 mm (Nuyttens & van de Pol, 2012).

Respiratory gating involves the delivery of treatment in a certain phase or interval of the breathing cycle (Verellen *et al*., 2007). This can be achieved either with the beam-on/off of the treatment machine synchronised with the patient's breathing, or with breath-hold techniques (Benedict, 2005). Gating techniques are more time-consuming than tracking techniques as only a part of the breathing cycle is beam-on time, but the treatment time can be decreased with breath holding.

In general, the probability distribution function of the breathing motion in the longitudinal direction, obtained from clinical data of liver tumours presented in Paper III and IV, shows a shift of the time-weighted mean position of the tumour towards more cranial locations corresponding to an exhale breathing phase. The time-weighted tumour position towards the exhale position has also been presented by others (Seppenwoolde *et al*., 2002). It was also shown that the longest time is *not* spent at the end-positions of the breathing cycle, as implicitly assumed when simulating a sinus-shaped motion (Lujan, Larsen, Balter, & Ten Haken, 1999). However, simulating breathing motion with a sinus curve is common, probably due to the simplicity to implement. It is reasonable to assume that breathing motions of liver tumours are applicable also for lung tumours, at least for lung tumours located in the lower parts of the lungs.

5.1.2 Deformations and tissue changes

Apart from positional changes of the tumour, the breathing also causes deformations of the tissues in the lungs and abdomen. In some rare cases, we have also observed deformation of the shape of the tumour. During a course of radiotherapy, the tumour and the surrounding tissues can change in volume and structure, due to the radiation, but also due to other patient-related issues (Tatekawa *et al*., 2014).

5.1.3 Baseline shift

Baseline shifts are defined as the differences in the tumour or OAR position relative to the skeleton between the treatment-planning CT and the treatment fractions (Worm *et al*., 2010). This can be caused by factors such as weight gain or loss, reduced or increased swellings, atelectasis, accumulation of pleural effusion, differences in abdominal content, or other patient-related factors. In SBRT, baseline shifts of the tumour are more often seen between the treatment-planning CT and the first treatment than in between the treatment fractions, since the time generally is longer between the former than the latter.

5.1.4 Breathing phase of the treatment-planning CT

There are different methods in use related to breathing for the choice of treatment-planning CT, and as the reference in online image-guidance at treatment. One is to use the time-averaged mid-ventilation phase images reconstructed from a 4DCT, alternatively to select the

phase of the 4DCT that best represents a mid-ventilation phase (Wolthaus *et al*., 2006). Another commonly used, but less accurate approach, is to use CT images that are taken in a random phase during free-breathing. In SBRT before online CBCT image-guidance was introduced and patient positioning was performed by means of the stereotactic coordinates, this random breathing phase introduced a systematic error which was accounted for by using CTV-to-PTV margins larger than or at least as large as the tumour breathing amplitude. With the use of online CBCT image-guidance, the CBCT image of the tumour is matched to the reference image of the tumour from the treatment-planning CT. The dose delivered to the tumour should therefore be close to the planned one with some residual uncertainties, while OAR not moving together with (or not moving to the same extent as) the tumour could potentially get a dose that differs considerably from the planned dose. The larger the breathing amplitude, the more impact this will have on the delivered dose to these OAR.

In Paper IV, the impact of the treatment-planning CT in a random breathing phase is considered in the estimation of delivered CTV doses for the time period before online image-guidance was available.

5.1.5 Structure delineation

The accuracy in delineation of the GTV and the CTV in the images used for treatment planning is of utmost importance. For delineation of the CTV, biological characteristics of the tumour and recurrence patterns should be taken into consideration (Dobbs & Landberg, 2003). Apart from the uncertainties in the target delineation, there are also uncertainties in the definition and outlining of OAR. The accuracy in the structure delineation might be limited by the image resolution and the slice thickness of the treatment-planning CT.

Steenbakkers *et al*. (2006) studied delineation variations of the GTV for Stage I-III NSCLC and concluded that even with the help of fused positron emission tomography (PET) and CT images the inter-observer variations were large compared to setup uncertainties and organ motion. The observer variation was reduced from 10 mm (standard deviation (std)) to 4 mm (std) comparing delineation on CT only with PET/CT. At the same time, Peulen *et al*. (2015) reported a variability in the GTV delineation of 2 mm (root-mean-square) at mid-ventilation planning CT for Stage I-II NSCLC, with smaller variations within the different institutions. Also, Mantel *et al*. (2013) suggest PET images to facilitate the tumour definition in comparison to radiation-induced fibrosis in a reirradiation setting.

5.1.6 Online image-guidance

Online image-guidance with soft-tissue tumour matching with CBCT or other imaging-systems is today the most commonly used method for fine-tuning the tumour localisation in SBRT, thus reducing the setup errors. The focus in the matching process is the repositioning of the tumour and to a minor extent the OAR. This might lead to larger uncertainties in the reproducibility of the surrounding OAR, compared to that of the target. These uncertainties must be considered if there is a risk of delivery of too high doses to OAR.

The image quality of the online image system, as well as that of the reference CT, is crucial for the accuracy of the matching of the CBCT and the reference CT images. A study by Sweeney *et al*. (2012) showed that with the use of 4D-CBCT in comparison with 3D-CBCT, both the target visibility and localisation were improved together with reduced inter-observer target localisation variability. They presented an average 3D difference of 2±1 mm (std) between matching with 4D-CBCT and 3D-CBCT.

5.1.7 Setup

Setup uncertainties can be divided into a systematic and a random component, as expressed by van Herk *et al*., describing the treatment preparation uncertainties and the treatment execution uncertainties, respectively (van Herk, Remeijer, Rasch, & Lebesque, 2000). The systematic setup uncertainty is caused by differences between patient positioning during the treatment-planning CT acquisition, and patient positioning at the treatment execution. It is defined as the mean deviation of positioning at all treatment fractions in comparison to the planned position, which is an unproblematic definition only in the case of an infinite or large number of fractions. The systematic setup uncertainty might be caused by misplaced setup tattoos or markers on the CT images, differences in setup routines between CT acquisition and treatment, or incorrectly calibrated lasers indicating the isocenter of the linac. The random setup uncertainty is due to variations in patient positioning from treatment to treatment, and is defined as the deviation in positioning from the mean, which can be caused by mobility of the skin with tattoos, patient movements (due to pain, uncomfortable treatment position, difficulties in keeping still), or different treatment staff using different routines.

In Paper IV the setup uncertainty was given a very specific meaning, in which the uncertainties in the CBCT matching and the breathing phase of the treatment-planning CT were considered separately. In a first step, systematic (Σ^2) and random (σ^2) variances of observed patient data of couch corrections after CBCT tumour match were corrected for the finite number of fractions in the observations, due to the treatment delivery in few fractions. From these, the setup variances for SBRT without online image-guidance were defined as:

$$\Sigma_{Setup}^2 = \Sigma_{FFC}^2 - \Sigma_{CTphase}^2 - \Sigma_{Match}^2 \quad (6)$$

$$\sigma_{Setup}^2 = \sigma_{FFC}^2 - \sigma_{Match}^2 \quad (7)$$

where *FFC*, *CTphase* and *Match*, denotes respectively finite fraction corrected, breathing phase at the treatment-planning CT and assumed residual setup uncertainty after online CBCT matching.

Literature data of setup uncertainties generally gives the observed couch correction data, not specifying the systematic and random components. The mean absolute 3D variation of observed couch corrections in Paper IV using the SBF was 5.8±3.3 mm. The magnitude of observed setup uncertainties differs between different immobilisation devices. Shah *et al*. (2013) compared the translational mean target position correction after online CBCT with

different devices used in SBRT: the Stereotactic Body Frame, the Alpha Cradle, the BodyFIX, a hybrid combining the Alpha Cradle with the BodyFIX vacuum sheet, a wing board, and no fixation device at all. The inter- and intra-fraction mean target position variations were shown to be smallest with the SBF, and largest with the hybrid device for the inter-fraction variations, and with no device or the wing board for the intra-fraction variations, see Table 4. Further, Foster *et al*. (2013) present inter-fractional variations of 7.4±4.0 mm and 7.3±4.1 mm for lung tumours treated without and with the abdominal compression, respectively, and intra-fractional variations of 1.3±1.5 mm and 1.7±2.0 mm, respectively, using the SBF with application of abdominal compression for patients with longitudinal tumour breathing motion >10 mm. Correcting only for translational positioning errors, Josipovic *et al*. (2012) have shown a residual rotational error below 4° for 97% of the patients, and below 3° for 91% of the patients, using a VacFix cushion (PAR Scientific A/S, Odense, Denmark) and knee support.

Table 4*: Inter-fraction setup variations and intra-fraction tumour position variations for the SBF and a few other selected immobilisation devices.*

Reference	Device	Mean ± std (mm)
Inter-fraction setup variation		
Paper IV	SBF	5.8 ± 3.3
Shah *et al*. (2013)	SBF	6.9 ± 5.2
Foster *et al*. (2013)	SBF without compression	7.4 ± 4.0
Foster *et al*. (2013)	SBF with compression	7.3 ± 4.1
Shah *et al*. (2013)	Hybrid device	12.6 ± 10.2
Intra-fraction tumour position variation		
Shah *et al*. (2013)	SBF	2.3 ± 1.4
Foster *et al*. (2013)	SBF without compression	1.3 ± 1.5
Foster *et al*. (2013)	SBF with compression	1.7 ± 2.0
Shah *et al*. (2013)	Wing board	3.3 ± 1.7
Shah *et al*. (2013)	No device	3.3 ± 2.2

std = standard deviation, SBF = stereotactic body frame

5.1.8 Machine geometry

Uncertainties in position and calibration of machine geometry might arise from factors such as the gantry angle, the collimator positions, the MLC positions, the isocenter stability, the source-skin distance (SSD) scale, the treatment couch position and movement, and the alignment of the setup lasers to the treatment isocenter. All these parameters must routinely be checked within the quality assurance programs.

5.1.9 Human factor

The human factor is also a cause of uncertainties. It is important to maintain consistent methods for patient positioning and treatment procedures (McKenzie *et al*., 2003), as well as education of staff and availability of supervision of experienced staff in the learning phase. However, it is a complex process and there are still inter-personal differences in the judgement of images at image-guidance, and a risk of miscommunication, which can be exacerbated by a high work-overload leading to stress and the risk of making mistakes.

5.2 Dosimetric uncertainties

Dosimetric uncertainties may arise to a minor extent from for example the conversion of CT data from Hounsfield Units (HU) to electron density, data transfer between different systems and output calibration of the treatment machine. More important for dosimetric uncertainties is the accuracy in the dose calculation.

5.2.1 Dose calculation

The different algorithms for dose calculation can be divided into three different categories; Type A, Type B and Type C, depending on the accuracy in dose calculation. Type A models are the simplest to which the Pencil Beam (PB) algorithms with longitudinal scaling for inhomogeneity corrections belong. Type B models also consider an approximation of the lateral distribution of the secondary particles, and use both longitudinal and lateral scaling for inhomogeneities. Examples of Type B models are the Analytical Anisotropic Algorithm (AAA) and the Collapsed Cone (CC) algorithms. Type C models are the most accurate models available and track each particle, such as the Monte Carlo (MC) method.

A particular difference between the algorithms, as stated above, is how tissue inhomogeneities are managed. This is especially a challenge for lung tumours where there are large tissue density inhomogeneities ranging from the chest wall and tumour to lung tissue. Compared to water-equivalent tissue density, the lower density in the lungs results in electronic disequilibrium at the lung/tumour interface with lower dose at the edges of the tumour as a result (Papiez, Moskvin, & Timmerman, 2005). For lung tumours treated in the early period of SBRT, during which PB algorithms were used, this might have led to an overestimation of the peripheral dose to the tumour.

Paper III illustrates a consequence on the dose distribution from the interface effect between lung and tumour tissue. Setup errors and breathing motion were simulated with the less accurate dose-shift and more accurate beam-shift methods. The beam-shift result shows that the photon fluence builds up dose within the denser tumour, and the dose “follows” the tumour with the breathing motion.

In a phantom study of planned tumour doses in lung SBRT, Aarup *et al*. (2009) concluded that PB algorithms overestimate the tumour dose, while the AAA and the CC algorithms both adequately calculate the tumour dose, compared to MC simulations. Ojala *et al*. compared three different algorithms (PB, AAA and Acuros XB) and MC simulations for four patient cases with SBRT of lung tumours (Ojala, Kapanen, Hyödynmaa, Wigren, & Pitkänen, 2014). They concluded from the comparison with the MC simulations that Acuros XB could be used as reference to evaluate the performance of the PB and the AAA algorithms. The results showed relatively large differences in mean dose to the PTV, especially for smaller PTV volumes, and smaller differences in the lung tissue. Largest PTV dose difference was observed for the PB algorithm, with differences above 5% and up to nearly 60%, while differences with the AAA algorithm generally were below 5% but up to 20%. According to

McCowan *et al*., calculations with AAA compared to CC result in a 2-5% lower lung dose, and up to 5% higher dose in the tissue where the radiation exits the lung (McCowan, Van Uytven, Van Beek, Asuni, & McCurdy, 2015).

Latifi *et al*. (2014) report statistically significant higher rates of local recurrences after SBRT of NSCLC calculated with PB compared to those calculated with CC; 21.5% (crude rate) with PB and 4.7% with CC. Both patient cohorts were treated with the same prescribed dose and planned with the same criterions, but with differences in median follow-up time (24 months for PB versus 17 months for CC) and image-guidance technique (stereoscopic radiographs with implanted markers for PB versus CBCT for CC). However, they concluded the difference in local recurrence to be due to the relative underdosage of lung tumours planned with PB. Bibault *et al*. (2015), on the other hand, did not observe any differences in local control, between patients planned with Type A or Type B algorithms in SBRT of lung cancer.

5.3 Strategies to account for uncertainties

5.3.1 Margin concept

To account for uncertainties, a CTV-to-PTV margin can be added to account for all relevant geometrical and dosimetric uncertainties in order to ensure the delivery of prescribed dose to the CTV with an acceptable probability (ICRU, 1993, 1999, 2010). Breathing motion may be accounted for by an ITV, which should encompass the extent of the tumour in all geometrical positions mainly due to breathing (ICRU, 1999, 2010). Around the ITV, an ITV-to-PTV margin is added to account for all uncertainties except breathing. However, the ITV concept has been shown to provide unnecessarily large margins (Wolthaus *et al*., 2008).

Another method to account for breathing motion is to create the treatment plan based on the time-weighted mid-ventilation breathing phase and add margins to include the tumour for a large part of the breathing cycle (Wolthaus *et al*., 2006). It is not required to fully include the whole extent of the breathing amplitude in the margin, since delivery of reduced doses in the extreme positions do not have any large impact on the overall dose (Engelsman, Damen, De Jaeger, van Ingen, & Mijnheer, 2001), especially if heterogeneous dose distribution is used. Sonke *et al*. (2009) have shown that smaller CTV-to-PTV margins are needed with the mid-ventilation approach compared to the resulting extent with the ITV concept.

The margin concept used at the Karolinska University Hospital is to apply CTV-to-PTV margins of at least 10 mm and 5 mm, in the longitudinal and the transversal directions respectively, or equal to the measured peak-to-peak amplitude. Results from Paper IV indicate that these margins can be decreased thanks to the introduction of online image-guidance while still maintaining the same population coverage probability as estimated for the era before online image-guidance was introduced.

Several methods of calculating the margin have been proposed, with inclusion of different uncertainties from centre- or patient-population specific data. Based on recommendations in the ICRU report 50 (ICRU, 1993), Stroom *et al*. performed convolution of the CTV location including systematic (Σ) and random (σ) geometrical uncertainties (Stroom, de Boer, Huizenga, & Visser, 1999). They proposed a CTV-to-PTV margin recipe of $M = 2.0\Sigma + 0.7\sigma$ to ensure delivery of at least 95% of the dose to 99% of the CTV on average. A commonly used CTV-to-PTV margin formula, later proposed by van Herk *et al*. (2000), is:

$$M = \alpha\Sigma + \beta\left(\sqrt{\sigma^2 + \sigma_p^2} - \sigma_p^2\right) \quad (8)$$

where σ_p is determined by the penumbra width and σ excludes the penumbra. With the formula constants α=2.5 and β=1.64 it is assured that 90% of the population receives a minimum CTV dose of at least 95% of the prescribed dose. Note that the formula constants α and β are not to be confused with the α and β values used for fractionation sensitivity. Peulen *et al*. (2015) suggested that α should be increased from 2.5 to 2.8-3.2 to include the GTV delineation variability. In the van Herk margin formula a few assumptions are made, such as treatment with many fractions, and spherical tumour or large tumour in comparison with the random uncertainties (van Herk *et al*., 2000). To account for breathing, van Herk *et al*. proposed to add the standard deviation of the breathing motion, calculated by 0.358 times the peak-to-peak breathing motion amplitude derived from a periodically function with a non-Gaussian probability distribution, as one of the random geometrical uncertainties (van Herk, Witte, van der Geer, Schneider, & Lebesque, 2003).

Any application of simple predicative margin recipes to SBRT must be considered speculative without detailed validation studies, due to the specific assumptions that must be made. However, such reasoning can be useful for getting a "feeling" for the magnitudes necessary. An estimate of the CTV-to-PTV margin for 0-30 mm peak-to-peak breathing amplitude will range between 3 mm and 6 mm in each direction from the CTV, using α=2.79 for the confidence level of 95% of the patients, and β=0.5 for dose prescription to the 67% isodose line extrapolated from data provided by van Herk *et al*. (2000). This also assumes a breathing motion amplitude factor of 0.358 (van Herk *et al*., 2003), a penumbra factor of σ_p=6.4 mm for lung tissue (Sonke *et al*., 2009), and systematic and random setup errors of 1 mm, approximately evaluated by Sweeney *et al*. (2012) to be the variation of 3D-CBCT matching compared to 4D-CBCT matching, ignoring all other uncertainties. With a penumbra factor of σ_p=3.2 mm for tumours located in soft tissue (van Herk *et al*., 2000; Witte, van der Geer, Schneider, Lebesque, & van Herk, 2004) the CTV-to-PTV margin will range between 3 mm and 7 mm. Adding a target delineation uncertainty of 1.5 mm, as proposed by Peulen *et al*. (2015) to vary between 1.2-1.8 mm for early stage NSCLC, for tumours in lung tissue, the CTV-to-PTV margin would range between 6 mm and 9 mm. Using the "worst case" assumption for the setup uncertainty with CBCT matching from Paper IV with a systematic error of 2.1 mm and a random error of 1.6 mm in the longitudinal direction, the CTV-to-PTV margin ranges between 6 mm and 9 mm, using a penumbra factor for lung tissue, without any

target delineation uncertainty. With further addition in the margin formula of correction of treatment in few fractions (Gordon & Siebers, 2007), the CTV-to-PTV margin ranges between 7 mm and 10 mm for 0-30 mm peak-to-peak breathing amplitude, for 3 fractions with the worst case setup assumption.

Grills *et al*. (2008) have calculated CTV-to-PTV margins for setup errors not including breathing motion, for SBRT of lung tumours using the SBF, of 9-13 mm without online image-guidance, of 1-2 mm with daily CBCT image-guidance, and of 2-4 mm with daily CBCT and including intra-fractional systematic tumour displacement. These calculations are based on a margin formula proposed by Yan *et al.* (2005), which is a generalisation of the margin formulae proposed by Stroom *et al.* (1999) and van Herk *et al*. (2000).

Sonke *et al*. (2009) calculated CTV-to-PTV margins, with the van Herk formula, for frameless SBRT of peripheral lung tumours with treatment planning on the mid-ventilation phase with prescription to the 80% isodose line using 4D-CBCT image-guidance. They included systematic and random setup errors of about 1 mm (std), systematic baseline errors of 2-3 mm and random errors of 1-2 mm, systematic and random intra-fraction uncertainties of 1-2 mm, delineation variability of 2 mm, and a breathing motion scaling factor of 0.36. Monte Carlo validation of the margins showed that CTV-to-PTV margins of 6-11 mm were adequate for 94% of the included cases with breathing motions of 2-28 mm. In a publication by Peulen *et al*. (2014), from the same study group, they imply that their margins will be decreased to a baseline of 5 mm in the lateral and the longitudinal directions and 6 mm in the vertical direction, due to estimation of smaller variations within a more recent and larger analysed patient cohort.

Bissonnette *et al*. calculated setup margins with the van Herk formula $M = 2.5\Sigma+0.7\sigma$, incorporating σ_p=3.2 mm in the constant in front of the σ (van Herk *et al*., 2000), including systematic and random setup uncertainties of 2-5 mm derived from an initial localisation CBCT, and of 1-2 mm from a second verification CBCT after couch correction (Bissonnette, Purdie, Higgins, Li, & Bezjak, 2009). The calculated margins reduced from 12-15 mm to 4-6 mm after the introduction of CBCT matching.

Despite the speculative nature of such estimates, a broad agreement emerges that the appropriate CTV-to-PTV margin without online image-guidance lies in the approximate range of 10-15 mm. This is reduced to somewhere below 10 mm with online imaging, with the precise estimates depending on the treatment and imaging techniques as well as the assumptions made. Note that the van Herk margin formulae rely on the convolution assumption. A more rigorous treatment of the problem for hypofractionated treatments therefore requires a different approach, such as probabilistic sampling (Monte Carlo method).

5.3.2 Dose-coverage probability and probabilistic treatment planning

The margin concept is population based and does not take into account the specific geometry of the individual patient. Dose-coverage probability is a way of accounting for geometrical uncertainties which consider the individual geometry of the patient in the optimisation process of the treatment planning (Gordon, Sayah, Weiss, & Siebers, 2010). From data of the distributions of geometrical uncertainties, a treatment series may be simulated by repeated sampling from the distributions followed by dose calculations to get a number of dose-volume histograms (DVHs) for a given structure. From the DVHs the dose coverage probability or a complete map of dose coverage probabilities (Figure 9a) can be obtained (Gordon *et al*., 2010). This information is used in probabilistic treatment planning and has been shown to have the potential to reduce dose to OAR while ensuring adequate target coverage, as compared to margin-based planning (Bohoslavsky, Witte, Janssen, & van Herk, 2013).

To obtain low statistical uncertainties in probabilistic planning hundreds or thousands of dose calculations are often necessary. The time overhead for such calculations can be prohibitive and simplifications such as the dose-shift approximation are often used. However, Tilly and Ahnesjö (2015) have developed a fast dose algorithm of dose coverage probability, accounting for dosimetric effects of translational geometrical uncertainties. This algorithm repeatedly applies setup uncertainties and intra-fractional motion with random samples to the pre-calculated primary and scatter dose components, before the final dose calculation.

In Paper IV, dose-volume coverage maps (Figure 9a) and the resulting tumour-specific dose coverage histograms for 98% of the CTV (indicated by the blue dashed line in Figure 9a) were retrospectively calculated for a population of tumours (Figure 9b). From the latter, a population-averaged dose coverage histogram was calculated (Figure 9c) in order to get a measure relevant for comparison to clinical outcome data.

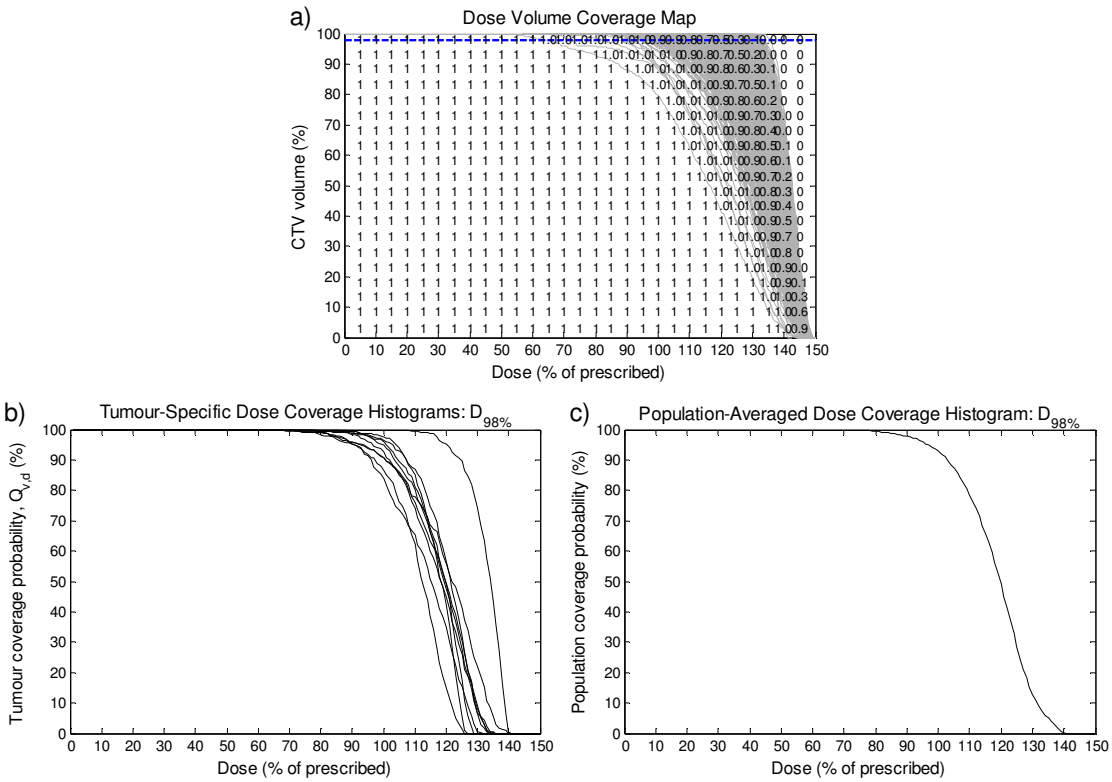

Figure 9*: An illustration of a) a dose-volume coverage map for one single tumour with the repeated DVHs, b) tumour-specific dose coverage histograms for 98% of the CTV volume for 10 different tumours, and c) a population-averaged dose coverage histogram for 98% of the CTV volume for the population of 10 different tumours.*

5.3.3 Estimation of delivered dose

Estimation of the delivered dose on a coverage probability basis was done in Paper IV. The delivered dose to the CTV, represented by the population coverage probability, was estimated considering breathing motion and setup or matching uncertainties, comparing soft-tissue image-guidance with pre-treatment verification CT (IG1) and online CBCT matching (IG2). A lower delivered dose to the CTV was shown for the IG1 method compared to the IG2 method, as shown in Figure 10, with different assumptions of setup and matching uncertainties. For the realistic case assumptions at a population coverage probability of 90%, the delivered $D_{98\%}$ to the CTV was at least 100% with IG1 and 117% with IG2, compared to the prescribed dose to the PTV periphery enclosed by the 67% isodose line. Compared to the planned $D_{98\%}$, the delivered $D_{98\%}$ to the CTV was at least 78% with IG1 and 93% with IG2.

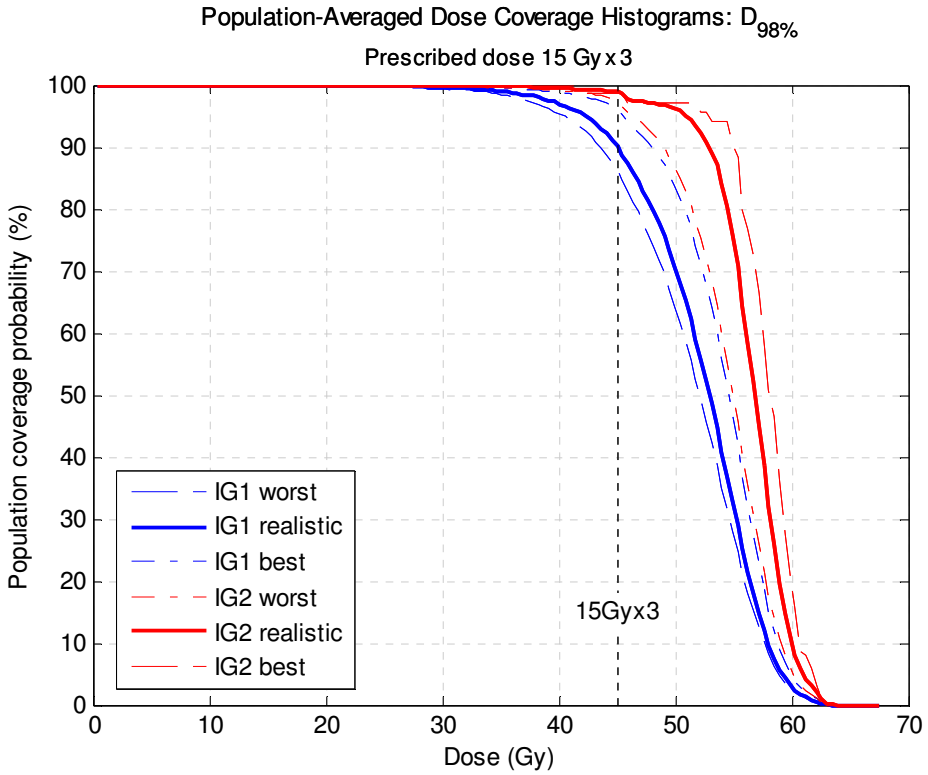

***Figure 10**: Population-averaged dose coverage histograms for two different image-guidance techniques (IG1 and IG2) and three different simulation scenarios (with worst, realistic and best case assumptions), estimated in Paper IV, here applied to the fractionation schedule of prescribed dose 15 Gy × 3 to the periphery of PTV corresponding to the 67% isodose line.*

The results presented in Figure 10 were estimated with a dose-shift (DSh) method with rigid shifts of an invariant dose distribution in relation to the tumour, considering breathing motion and setup errors. This approximate method has previously been used by others in the calculation of dose coverage probabilities (Bohoslavsky *et al.*, 2013; Gordon *et al.*, 2010; Moore, Gordon, Anscher, Silva, & Siebers, 2012). The accuracy of this method, for the particular case of lung tumours, was investigated in Paper III by comparing it to a beam-shift (BSh) method with recalculation of the dose distribution in the different geometrical positions resulting from setup errors and breathing motion. Here, the BSh method was considered the gold standard to which the DSh method was benchmarked. However, the validity of the BSh method used as reference might be questioned, *i.e.* whether the BSh approach can be expected to be accurate, or even more accurate than the DSh method. It is reasonable to assume that the BSh method is accurate for pure setup errors. An advantage of the BSh method is that the dose tracking effects due to differences in density between the tumour and its surrounding is included, which is not the case for the DSh method. However, the BSh method does not account for anatomy deformations due to breathing, nor for anatomy deformations due to baseline shifts of the tumour location between the treatment-planning CT and the dose delivery. To simulate breathing using a rigid shift of a patient is a crude model, but it has been demonstrated to be generally accurate to better than 2% even with extreme breathing amplitudes (Mexner *et al.*, 2007; Sonke *et al.*, 2009). Further, in this study, it was

observed that for breathing amplitudes within the CTV-to-PTV margins, breathing makes little difference to the delivered dose in the CTV.

The purpose of Paper IV was to compare the two different methods IG1 and IG2 by means of the population-averaged dose coverage histogram. However, for evaluation of dose-response data, it would be more relevant to use the tumour-specific dose coverage histogram data and to model the patient-individual response with delivered dose, rather than the population-averaged. Patient-individual reconstruction of delivered dose, based on 4DCT data, has been done by Guckenberger *et al*. and Admiraal *et al*. They transferred the treatment plan to each of the breathing phases in the 4DCT and recalculated the dose to estimate the delivered dose considering breathing motion for lung tumours treated with SBRT (Admiraal, Schuring, & Hurkmans, 2008; Guckenberger *et al*., 2007). Admiraal *et al*. (2008) showed that the accumulated CTV dose generally was equal to or higher than the planned PTV dose, except in the high-dose region of the DVH comparison. Guckenberger *et al*. (2007) did not find any significant GTV dose difference with the tumour located in its end-exhalation, end-inhalation or mid-ventilation phase. Increased accuracy in the delivered-dose estimation, including also the setup errors, could be achieved with the usage of 4D-CBCT.

Further accuracy in estimation of the delivered dose would require online registration of the patient anatomy during the complete treatment course, followed by recalculation of the dose. A possible method in this direction is the use of the electronic portal imaging device (EPID) during delivery. Berbeco *et al*. (2008) retrospectively estimated the delivered dose adjusting the beams in the treatment plan to the tumour shift estimated from each projection of the EPID images acquired during treatment. The method was further developed with the creation of 3D images for different time-points from the EPID images acquired, based on the patient-specific motion derived from 4DCT (Cai *et al*., 2015). This method was shown to be as good as the accumulated dose calculated on the 4DCT phases for *regular* breathing motion, but better for *irregular* breathing motions. Another use of the EPID images was implemented by McCowan *et al*. (2015), who created a model for reconstruction of the delivered dose using the EPID images acquired during treatment and Monte Carlo simulations of the fluence.

A further alternative for estimating the delivered dose is using the target-position information during treatment intended for tumour tracking. Estimation of delivered dose has been based on tumour implanted electromagnetic transponder signals (Keall *et al*., 2014; Poulsen *et al*., 2012). However, kV images (Colvill *et al*., 2016), or magnetic resonance (MR) imaging on a MR-fused treatment machine (Menten *et al*., 2016), could potentially also be used.

6 Summary of papers

6.1 Paper I: Toxicity after reirradiation of pulmonary tumours with stereotactic body radiotherapy

Purpose: The purpose of this study was to evaluate the feasibility of reirradiation with SBRT for lung tumours after previous SBRT treatment in an overlapping region. The outcome was retrospectively evaluated with regard to toxicity, local control and survival.

Materials and Methods: Included were 29 patients reirradiated for 32 tumours, out of whom 11 had centrally- and 18 had peripherally-located tumours. The median follow-up time was 12 months (1-97 months). Reirradiation was defined as more than 50% overlap between the previously and new PTVs. Toxicity was retrospectively evaluated from the patients' medical records according to CTCAE version 3.

Results: The mean time between the first treatment and reirradiation was 14 months (5-54 months). Grade 3-4 adverse events were observed 14 times in 8 patients. Larger tumour volumes and central location were correlated to more severe toxicity. Three (27%) of the patients with centrally located lung tumours died due to bleeding, while no grade-5 toxicity was observed for patients with peripherally located tumours. No association was found between MLD and lung toxicity. Local control was 52% at 5 months after reirradiation, with poorer local control for larger tumours. The Kaplan-Meier estimated survival at 1, 2 and 3 years from the time of reirradiation were 59%, 43% and 23%, respectively.

Conclusion: It was concluded that reirradiation with SBRT in a similar location to one previously treated with SBRT was feasible with low rates of toxicity for patients with peripheral lung tumours, while caution should be taken for patients with central lung tumours due to the risk of increased severe toxicity.

6.2 Paper II: Retrospective cohort study of bronchial doses and radiation-induced atelectasis after stereotactic body radiation therapy of lung tumors located close to the bronchial tree

Purpose: In this study, a dose-response relationship for radiation-induced atelectasis and bronchial doses after SBRT treatment close to the bronchi was evaluated.

Materials and Methods: Retrospectively evaluated were 74 patients with tumours located close to the main, lobar or segmental bronchi. Doses to the bronchi were obtained from DVHs for maximum point dose as well as the dose to six different volumes ranging from 0.1 cm^3 to 2.0 cm^3. To account for different fractionation schedules, doses were recalculated to EQD_2 with both the LQ and the USC models. Estimations of dose-incidence curves were performed using the lognormal accelerated failure time model, with a parametric model for the hazard function.

Results and Conclusions: Eighteen patients (24%) developed atelectasis considered to be induced by radiation, at a median of 8 months (1-30 months) after treatment. A significant dose-response relationship was found between atelectasis and the high-dose volume of the bronchi. For the 64 patients with data available on $D_{0.1cm3}$, the median $D_{0.1cm3}$ of the bronchi was EQD_2=210 Gy_3 (mean 213 Gy_3, range 98-293 Gy_3) (LQ model, α/β=3 Gy) for patients that developed atelectasis, and EQD_2=105 Gy_3 (mean 124 Gy_3, range 20-279 Gy_3) for patient that did not. The total incidence of atelectasis (without taking the time aspect into account) was 0% at bronchial $D_{0.1cm3}$ in EQD_2 <80 Gy_3 (0/16 patients), 13% between 80-145 Gy_3 (2/16 patients), 25% between 145-190 Gy_3 (4/16 patients), and 56% at bronchial $D_{0.1cm3}$ ≥190 Gy_3 (9/16 patients). None of the patients with bronchial $D_{0.1cm3}$ values below EQD_2=98 Gy_3 developed an atelectasis, which means that no atelectasis was observed below bronchial doses corresponding to 11.3 Gy × 3, 8.5 Gy × 5, or 6.4 Gy × 8. These values may be used as dose constraints in treatment planning. The estimated incidence of atelectasis at 1, 2 and 3 years, respectively, was 3%, 8% and 13% at a bronchial $D_{0.1cm3}$ of EQD_2=100 Gy_3, 10%, 21% and 31% at EQD_2=150 Gy_3, and 25%, 42% and 53% at EQD_2=200 Gy_3.

6.3 Paper III: Accuracy of the dose-shift approximation in estimating the delivered dose in SBRT of lung tumours considering setup errors and breathing motions

Purpose: The aim of this study was to evaluate the accuracy of a dose-shift (DSh) approximation, with shifts of the planned static dose matrix, when estimating the delivered CTV dose considering setup errors and breathing motions of SBRT treated lung tumours. This method was compared with a more accurate beam-shift (BSh) method, with shifts of the beams/isocenter and recalculation of the dose distribution at different geometrical positions.

Materials and Methods: Ten representative patients treated with SBRT using static fields for ten lung tumours were included, selected to represent the variety of lung tumours treated at our clinic with respect to location in the lungs, tumour size, tumour shape and tumour density. An in-house developed toolkit within a treatment planning system allowed to: (i) shift a *precalculated* dose matrix according to a setup error and averaged over shifts of multiple phases of a breathing trace (the DSh method), or (ii) apply setup error and averaged over shifts of multiple phases as beam shifts with a *recalculation* of the treatment plan in each geometrical position (the BSh method). In both (i) and (ii) a series of setup errors (up to 10 mm) and breathing amplitudes (up to 10 mm in the longitudinal and 5 mm in the transversal directions) were simulated. From data retrieved from the DVHs of the CTV, dose and volume differences between the DSh and the BSh methods were evaluated in terms of $D_{98\%}$, $D_{50\%}$ and $D_{2\%}$.

Results and Conclusions: The results showed that the DSh method generally underestimates the delivered dose compared to the BSh method. To estimate the delivered dose for a particular patient, it is advisable to use the BSh method for increased accuracy. However, the

DSh method is computationally easier to implement, and averaged over a patient population this method is estimated to underestimate the delivered minimum CTV dose ($D_{98\%}$) to about 1% with setup shifts up to 10 mm. The root-mean-square discrepancy for such large shifts was around 4%. However, for more realistic setup shifts when using online image-guidance, of up to 5 mm, the root-mean-square discrepancy decreased to approximately 2%. For setup shifts up to 5 mm, the mean and root-mean-square dose discrepancies were broadly similar for $D_{50\%}$ and $D_{2\%}$. It was therefore concluded that averaged over a group of patients the DSh approximation has an acceptable error.

6.4 Paper IV: Estimation of delivered dose to lung tumours considering setup uncertainties and breathing motion in a cohort of patients treated with SBRT

Purpose: In this study the purpose was to estimate the delivered dose (dose coverage probability) to the CTV for a population of patients, taking into account setup errors, matching uncertainties and breathing motions. Comparison of delivered dose was made between two different volumetric image-guidance techniques with the capability to discern soft-tissue; pre-treatment verification CT (IG1) (standard before the introduction of online image-guidance), and online image-guidance with CBCT (IG2).

Materials and Methods: Delivered dose was retrospectively simulated for 50 consecutive patients treated with SBRT for 69 lung tumours. Simulations were performed with the DSh method using an in-house developed program that shifted and weighted the static dose distribution according to a breathing trace scaled with patient-specific amplitudes. Applied were also systematic and random setup (IG1) and matching (IG2) errors, sampled from normal distributions. These errors were obtained from clinical data with assumptions relevant for IG1 as well as IG2, for a best, a worst and a more realistic scenario. The realistic scenario was based on literature values for matching errors, while the best and worst scenarios constituted a plausible envelope around. The accumulated DVH for the CTV was calculated, and the simulations were repeated 500 times for each tumour. From the set of 500 different DVHs, a tumour-specific dose coverage histogram was calculated with tumour coverage probabilities of the CTV at different dose levels. Further, population-averaged dose coverage histograms were calculated as the mean of the tumour-specific dose coverage histograms for all tumours, providing population coverage probabilities of the CTV at different dose levels. Moreover, dose-population histograms were calculated at different tumour coverage probabilities as the percentage of all tumours achieving different dose levels. This was repeated for each scenario for IG1 and IG2.

Results: Averaged over the tumours, prescribed dose to the periphery of the PTV was delivered to 98% of the CTV with a population coverage probability of 86-96% (range between worst and best scenario, realistic scenario: 90%) using IG1, and 97-99% (realistic scenario: 99%) using IG2. For a population coverage probability of 90%, $D_{98\%}$ to the CTV was at least 78% and 93% of the planned $D_{98\%}$, with IG1 and IG2 realistic scenarios

respectively. For IG1 in the realistic scenario, 67% of tumours had a tumour coverage probability of at least 90% at the prescribed dose, *i.e.* $D_{98\%}$ exceeded the prescribed dose in at least 90% of simulations for two-thirds of the tumours. For IG2 in the realistic scenario, 99% of tumours achieved that same tumour coverage probability at the prescribed dose.

Conclusions: On average, the minimum dose delivered to the CTV increased with the use of online CBCT image-guidance, compared to the use of pre-treatment verification CT. A substantial part of the tumours might have received a dose below the prescribed dose before the introduction of online image-guidance. However, the increase in dose coverage with the implementation of online image-guidance has not yet been reflected in improved clinical outcome of local control, implying that the level of dose coverage is not the only explanation for local progression.

7 Main conclusions

Paper I: Reirradiation with SBRT after previous SBRT treatment in an overlapping region is feasible with acceptable toxicity levels for peripherally located lung tumours, but should be performed with caution for centrally located lung tumours due to increased risk of severe toxicity.

Paper II: There is a significant dose-response relationship between radiation-induced atelectasis and the dose to the high-dose region of the bronchi. However, further research to find the maximum tolerable dose for the bronchi is needed.

Paper III: To consider geometrical uncertainties when estimating the delivered dose to the tumour from the treatment plan, the use of the dose-shift approximation is generally unsuitable when precise dose estimates are desired for specific patients but is acceptable when applied to a population of patients.

Paper IV: Comparing estimated delivered doses to the tumour considering breathing motion and setup uncertainties with two different image-guidance techniques, the formerly used verification CT and the presently used online CBCT matching, showed that with the online CBCT matching the delivered dose to the tumour was increased considerably. This implies that with CBCT matching, local tumour control may be higher, if there is a dose-response at these dose levels. If not, the CTV-to-PTV margins could safely be decreased to lower the dose to surrounding OAR and thereby reduce the probability of radiation-induced toxicity.

8 Future research

There are many questions that remain within the field of SBRT. A deeper understanding of the relationship between treatment parameters and the outcome is needed, both in terms of local control and toxicity. Therefore, there is a need for improved systematic collection of follow-up data: this is the "clinical" end of the SBRT issue. However, the relationship between planned and delivered dose is poorly known. This requires many of the tools and concepts developed by physicists in IGRT over the last decades, as well as new ones, to be applied to dose calculations: this is the "physics" end of the SBRT issue. In this thesis, the issue was approached from both ends. Further research is needed to be able to relate delivered dose to treatment outcome. Here follows some questions within the area of this thesis where I see a need for future research.

It is important to get an improved knowledge as to whether increased tumour coverage probability ($D_{98\%}$) increases the rate of local tumour control, at the prescribed doses commonly used in SBRT. If that is not the case, the local control rather depends on other factors. Minimum dose to the CTV may not be the most decisive factor but other aspects of the dose distribution within the CTV, or factors that may be tumour-individual and connected to the distribution of radiation sensitivity within the CTV. If, on the other hand, it can be shown that $D_{98\%}$ is the most decisive factor for local tumour control, then the magnitude of the CTV-to-PTV margin will be highly important, to which the minimisation of systematic geometrical errors is the dominating component. A factor of uncertainty related to the probability of local control is the accuracy in the delineation of the CTV, and what dose is required for volumes with suspect tumour growth with low tumour-cell density, outside the GTV at the periphery of the target.

With regard to toxicity from SBRT, the CTV-to-PTV margin should be as small as possible to minimise dose to surrounding tissues. Improved knowledge of delivered dose to OAR for improved dose-response relations for OAR is important. The use of these improved relations would also require detailed knowledge of geometrical uncertainties, to be applied in probabilistic treatment planning. Furthermore, to what extent improved dose-delivery methods may reduce dose to OAR is important to evaluate. These methods may include improved dose distributions with photons or maybe also protons. It is also of importance to evaluate delivery methods such as gating and tracking, and what value these methods adds, considering the lower importance of random geometrical uncertainties for the CTV-to-PTV margin needed.

Acknowledgements

I would like to express my deepest gratitude to **everyone around me** that in various direct or indirect ways have supported me in this work, especially I would like to acknowledge:

Ingmar Lax, my principal supervisor, that with your commitment and involvement has introduced me to and support me in the world of clinical radiotherapy physics and especially SBRT, and for pushing me to think by myself and for helping me with your deliberated and clear mind when I am stuck

Peter Wersäll, my co-supervisor, for your friendly and dedicated way to help me with all clinical aspects of research and radiotherapy, and for the comfort and pleasure of having you in the everyday clinical practice and development of SBRT

Gavin Poludniowski, my co-supervisor, for your deep commitment and broad knowledge in physics and research, and for being a reliable and dedicated support in the development of our research and my knowledge and thinking

Jan Nyman, my co-supervisor, for your expertise and your commitment in helping me with clinical aspects of radiotherapy of lung tumours

Giovanna Gagliardi, my mentor, for introducing me to clinical radiotherapy physics and supporting me in professional and psychosocial considerations, and for giving me the opportunity to do my PhD and to focus on research during these years

Elias Lindbäck, my colleague and co-author, for interesting discussions and nice collaboration, and for supporting me and keeping me company during late evening measurements

Eva Onjukka, my colleague, co-author and classmate, for being by my side from the first day in medical physics, for fruitful discussions and collaborations, for supporting conversations about work and life, and for the company during endless night hours with Helax-TMS

Karin Lindberg, my colleague and co-author, for fruitful discussions about toxicities and medical issues, and profitable collaborations in SBRT

Heike Peulen, my Dutch colleague and co-author, for fun, interesting and profitable collaborations

Pia Baumann, my former colleague and co-author, for introducing me to the medical aspects of radiotherapy and especially SBRT, and for your inspiring driving force in research

Owe Tullgren, *in memoriam*, my former colleague and co-author, for challenging questions and fruitful collaboration

Rolf Lewensohn, my colleague and co-author, for wise discussions on clinical aspects of radiotherapy, and for your commitment to developing our research in SBRT

Ninni Drugge and **Karl-Axel Johansson**, my colleagues and co-authors in Gothenburg, for practical support with inclusion of patients treated at Sahlgrenska University Hospital

Jan-Olov Persson, my co-author, for all the support, guidance and discussions in statistics

Ricardo Palanco-Zamora, my colleague, for fruitful and inspiring discussions and collaborations in research aspects, radiotherapy physics, and clinical practice

Tobias Pommer, my colleague, for valuable discussions and feedback regarding clarity in reporting and presenting research results

Annette Fransson Andreo Hernandez, head of my department, for seeing every single one of us and for giving me the opportunity to do my PhD and focus on research

The **Stockholm and Nordic SBRT study group**, for interesting and fruitful discussions, collaborations and exchange of knowledge and experiences in SBRT

All **my colleagues** at the Department of Radiotherapy Physics and Engineering and at the Radiotherapy Department, for all the help and support in everything from technical issues with Aria, TMS, the linear accelerators, the CT scanner and fixations, to complicated decisions and real-life experiences, and fruitful and inspiring discussions

All **my PhD colleagues** at the Department of Medical Radiation Physics and the Department of Oncology-Pathology, for support, exchange and discussions about PhD related issues and during demanding PhD courses

The **Department of Medical Physics** and **Stockholm Cancer Society** for financial support

All **my psychologists, mentors and life coaches**, especially **Torkild Sköld**, for supporting me in emotional and psychological challenges and in developing myself during these years

My friends, for letting me escape to long distance running, small cabins far away from civilisation, spa weekends, “fika” sessions, iMessage therapy, stomach-aching laughter and deep conversations about life

My family and relatives, for always being a support and believing in me, for challenging my limits, for being a security to always rely on and fall back on, for creating opportunities to large lively gatherings in my life

Daniel, my love, for always being there, my support in everyday life, in all my ups and downs, and in the struggle of developing my true self, for all the inspiring discussions about all aspects of life, for filling my heart with joy, for being my closest friend and future

Bibliography

Aarup, L. R., Nahum, A. E., Zacharatou, C., Juhler-Nøttrup, T., Knöös, T., Nyström, H., . . . Korreman, S. S. (2009). The effect of different lung densities on the accuracy of various radiotherapy dose calculation methods: implications for tumour coverage. *Radiotherapy and Oncology, 91*(3), 405-414. doi: 10.1016/j.radonc.2009.01.008

Adebahr, S., Collette, S., Shash, E., Lambrecht, M., Le Pechoux, C., Faivre-Finn, C., . . . Nestle, U. (2015). LungTech, an EORTC Phase II trial of stereotactic body radiotherapy for centrally located lung tumours: a clinical perspective. *British Journal of Radiology, 88*(1051), 20150036. doi: 10.1259/bjr.20150036

Admiraal, M. A., Schuring, D., & Hurkmans, C. W. (2008). Dose calculations accounting for breathing motion in stereotactic lung radiotherapy based on 4D-CT and the internal target volume. *Radiotherapy and Oncology, 86*(1), 55-60. doi: 10.1016/j.radonc.2007.11.022

Allibhai, Z., Taremi, M., Bezjak, A., Brade, A., Hope, A. J., Sun, A., & Cho, B. C. (2013). The impact of tumor size on outcomes after stereotactic body radiation therapy for medically inoperable early-stage non-small cell lung cancer. *International Journal of Radiation Oncology Biology Physics, 87*(5), 1064-1070. doi: 10.1016/j.ijrobp.2013.08.020

Baba, F., Shibamoto, Y., Tomita, N., Ikeya-Hashizume, C., Oda, K., Ayakawa, S., . . . Sugie, C. (2009). Stereotactic body radiotherapy for stage I lung cancer and small lung metastasis: evalutaion of an immobilization system for suppression of respiratory tumor movement and preliminary results. *Radiation Oncology, 4*, 15. doi: 10.1186/1748-717X-4-15

Baschnagel, A. M., Mangona, V. S., Robertson, J. M., Welsh, R. J., Kestin, L. L., & Grills, I. S. (2013). Lung metastases treated with image-guided stereotactic body radiation therapy. *Clinical Oncology, 25*(4), 236-241. doi: 10.1016/j.clon.2012.12.005

Baumann, P., Nyman, J., Høyer, M., Wennberg, B., Gagliardi, G., Lax, I., . . . Lewensohn, R. (2009). Outcome in a prospective phase II trial of medically inoperable stage I non-small-cell lung cancer patients treated with stereotactic body radiotherapy. *Journal of Clinical Oncology, 27*(20), 3290-3296. doi: 10.1200/JCO.2008.21.5681

Baumann, P., Nyman, J., Lax, I., Friesland, S., Høyer, M., Rehn Ericsson, S., . . . Lewensohn, R. (2006). Factors important for efficacy of stereotactic body radiotherapy of medically inoperable stage I lung cancer. A retrospective analysis of patients treated in the Nordic countries. *Acta Oncol, 45*(7), 787-795. doi: 10.1080/02841860600904862

Benedict, S. H. (2005). Immobilization, localization, and repositioning methods in stereotactic body radiation therapy. In B. D. Kavanagh & R. D. Timmerman (Eds.), *Stereotactic body radiation therapy*. Philadelphia, USA: Lippincott Wiliams & Wilkins.

Bentzen, S. M. (2009). Dose-response relationships in radiotherapy. In M. Joiner & A. van der Kogel (Eds.), *Basic clinical radiobiology* (4th ed.). Boca Raton, FL, USA: CRC Press.

Berbeco, R. I., Hacker, F., Zatwarnicki, C., Park, S. J., Ionascu, D., O'Farrell, D., & Mamon, H. J. (2008). A novel method for estimating SBRT delivered dose with beam's-eye-view images. *Medical Physics, 35*(7), 3225-3231. doi: 10.1118/1.2938514

Bernstein, C., Prasad, A. R., Nfonsam, V., & Bernstein, H. (2013). DNA damage, DNA repair and cancer. In C. Chen (Ed.), *New research directions in DNA repair*. InTech. Available at: http://www.intechopen.com/books/new-research-directions-in-dna-repair/dna-damage-dna-repair-and-cancer.

Bezjak, A., Bradley, J., Gaspar, L., Timmerman, R. D., Papiez, L., Gore, E., . . . Normolle, D. (2014). Seamless phase I/II study of stereotactic lung radiotherapy (SBRT) for early stage, centrally located, non-small cell lung cancer (NSCLC) in medically inoperable patients: Radiation Therapy Oncology Group 0813. Available at: http://www.rtog.org.

Bezjak, A., Paulus, R., Gaspar, L. E., Timmerman, R. D., Straube, W. L., Ryan, W. F., . . . Choy, H. (2016). Primary Study Endpoint Analysis for NRG Oncology/RTOG 0813 Trial of Stereotactic Body Radiation Therapy (SBRT) for Centrally Located Non-Small Cell Lung Cancer (NSCLC). *International Journal of Radiation Oncology Biology Physics, 94*(1), 5-6. doi: 10.1016/j.ijrobp.2015.10.040

Bibault, J. E., Mirabel, X., Lacornerie, T., Tresch, E., Reynaert, N., & Lartigau, E. (2015). Adapted Prescription Dose for Monte Carlo Algorithm in Lung SBRT: Clinical Outcome on 205 Patients. *Plos One, 10*(7), e0133617. doi: 10.1371/journal.pone.0133617

Bissonnette, J. P., Purdie, T. G., Higgins, J. A., Li, W., & Bezjak, A. (2009). Cone-beam computed tomographic image guidance for lung cancer radiation therapy. *International Journal of Radiation Oncology Biology Physics, 73*(3), 927-934. doi: 10.1016/j.ijrobp.2008.08.059

Blomgren, H., Lax, I., Göransson, H., Kraepelien, T., Nilsson, B., Näslund, I., . . . Tilikidis, A. (1998). Radiosurgery for tumors in the body: clinical experience using a new method. *Journal of Radiosurgery, 1*, 63-74. doi: 10.1023/B:JORA.0000010880.40483.c4

Blomgren, H., Lax, I., Näslund, I., & Svanström, R. (1995). Stereotactic high dose fraction radiation therapy of extracranial tumors using an accelerator. Clinical experience of the first thirty-one patients. *Acta Oncol, 34*(6), 861-870. doi: 10.3109/02841869509127197

Boda-Heggemann, J., Frauenfeld, A., Weiss, C., Simeonova, A., Neumaier, C., Siebenlist, K., . . . Lohr, F. (2014). Clinical outcome of hypofractionated breath-hold image-guided SABR of primary lung tumors and lung metastases. *Radiation Oncology, 9*, 10. doi: 10.1186/1748-717X-9-10

Bohoslavsky, R., Witte, M. G., Janssen, T. M., & van Herk, M. (2013). Probabilistic objective functions for margin-less IMRT planning. *Physics in Medicine and Biology, 58*(11), 3563-3580. doi: 10.1088/0031-9155/58/11/3563

Bral, S., Gevaert, T., Linthout, N., Versmessen, H., Collen, C., Engels, B., . . . Storme, G. (2011). Prospective, risk-adapted strategy of stereotactic body radiotherapy for early-stage non-small-cell lung cancer: results of a Phase II trial. *International Journal of Radiation Oncology Biology Physics, 80*(5), 1343-1349. doi: 10.1016/ j.ijrobp.2010.04.056

Cai, W., Hurwitz, M. H., Williams, C. L., Dhou, S., Berbeco, R. I., Seco, J., . . . Lewis, J. H. (2015). 3D delivered dose assessment using a 4DCT-based motion model. *Medical Physics, 42*(6), 2897-2907. doi: 10.1118/1.4921041

Chang, J. Y., Senan, S., Paul, M. A., Mehran, R. J., Louie, A. V., Balter, P., . . . Roth, J. A. (2015). Stereotactic ablative radiotherapy versus lobectomy for operable stage I non-small-cell lung cancer: a pooled analysis of two randomised trials. *Lancet Oncology, 16*(6), 630-637. doi: 10.1016/S1470-2045(15)70168-3

Chaudhuri, A. A., Tang, C., Binkley, M. S., Jin, M., Wynne, J. F., von Eyben, R., . . . Diehn, M. (2015). Stereotactic ablative radiotherapy (SABR) for treatment of central and ultra-central lung tumors. *Lung Cancer, 89*(1), 50-56. doi: 10.1016/j.lungcan.2015.04.014

Chik, Y. K., Cheung, K. M., Lam, H. C., Kwan, C. K., & Au, J. S. K. (2015). Survival outcomes of Stereotactic body radiotherapy for early-staged non-small cell lung cancer: a comparison between different doses. *Journal of Thoracic Oncology, 10*(9), S679-S680. Available at: http://www.jto.org/article/S1556-0864(1516)30012-30010/pdf.

Colvill, E., Booth, J., Nill, S., Fast, M., Bedford, J., Oelfke, U., . . . Keall, P. (2016). A dosimetric comparison of real-time adaptive and non-adaptive radiotherapy: A multi-institutional study encompassing robotic, gimbaled, multileaf collimator and couch tracking. *Radiotherapy and Oncology, 119*(1), 159-165. doi: 10.1016/j.radonc.2016.03.006

Dance, D., & Alm Carlsson, G. (2007). Interactions of photons with matter. In P. Mayles, A. Nahum & J.-C. Rosenwald (Eds.), *Handbook of radiotherapy physics - Theory and practice*. Boca Raton, FL, USA: CRC Press Taylor & Francis Group.

Dobbs, J., & Landberg, T. (2003). Clinical overview of geometric uncertainties in radiotherapy *Geometric uncertainties in radiotherapy - Defining the planning target volume*. London, UK: The British Institute of Radiology.

Duijm, M., Schillemans, W., Aerts, J. G., Heijmen, B., & Nuyttens, J. J. (2016). Dose and Volume of the Irradiated Main Bronchi and Related Side Effects in the Treatment of Central Lung Tumors With Stereotactic Radiotherapy. *Seminars in Radiation Oncology, 26*(2), 140-148. doi: 10.1016/j.semradonc.2015.11.002

Eisenhauer, E. A., Therasse, P., Bogaerts, J., Schwartz, L. H., Sargent, D., Ford, R., . . . Verweij, J. (2009). New response evaluation criteria in solid tumours: revised RECIST guideline (version 1.1). *Eur J Cancer, 45*(2), 228-247. doi: 10.1016/j.ejca.2008.10.026

Engelsman, M., Damen, E. M., De Jaeger, K., van Ingen, K. M., & Mijnheer, B. J. (2001). The effect of breathing and set-up errors on the cumulative dose to a lung tumor. *Radiotherapy and Oncology, 60*(1), 95-105. doi: 10.1016/S0167-8140(01)00349-8

Fakiris, A. J., McGarry, R. C., Yiannoutsos, C. T., Papiez, L., Williams, M., Henderson, M. A., & Timmerman, R. (2009). Stereotactic body radiation therapy for early-stage non-small-cell lung carcinoma: four-year results of a prospective phase II study. *International Journal of Radiation Oncology Biology Physics, 75*(3), 677-682. doi: 10.1016/j.ijrobp.2008.11.042

Foster, R., Meyer, J., Iyengar, P., Pistenmaa, D., Timmerman, R., Choy, H., & Solberg, T. (2013). Localization accuracy and immobilization effectiveness of a stereotactic body

frame for a variety of treatment sites. *International Journal of Radiation Oncology Biology Physics, 87*(5), 911-916. doi: 10.1016/j.ijrobp.2013.09.020

Fowler, J. F., Tome, W. A., & Welsh, J. S. (2005). Estimation of required doses in sterotactic body radiation therapy. In B. D. Kavanagh & R. D. Timmerman (Eds.), *Stereotactic body radiation therapy*. Philadelphia, USA: Lippincott Wiliams & Wilkins.

Gordon, J. J., Sayah, N., Weiss, E., & Siebers, J. V. (2010). Coverage optimized planning: Probabilistic treatment planning based on dose coverage histogram criteria. *Medical Physics, 37*(2), 550-563. doi: 10.1118/1.3273063

Gordon, J. J., & Siebers, J. V. (2007). Convolution method and CTV-to-PTV margins for finite fractions and small systematic errors. *Physics in Medicine and Biology, 52*(7), 1967-1990. doi: 10.1088/0031-9155/52/7/013

Grills, I. S., Hope, A. J., Guckenberger, M., Kestin, L. L., Werner-Wasik, M., Yan, D., . . . Belderbos, J. (2012). A collaborative analysis of stereotactic lung radiotherapy outcomes for early-stage non-small-cell lung cancer using daily online cone-beam computed tomography image-guided radiotherapy. *Journal of Thoracic Oncology, 7*(9), 1382-1393. doi: 10.1097/JTO.0b013e318260e00d

Grills, I. S., Hugo, G., Kestin, L. L., Galerani, A. P., Chao, K. K., Wloch, J., & Yan, D. (2008). Image-guided radiotherapy via daily online cone-beam CT substantially reduces margin requirements for stereotactic lung radiotherapy. *International Journal of Radiation Oncology Biology Physics, 70*(4), 1045-1056. doi: 10.1016/j.ijrobp.2007.07.2352

Grills, I. S., Mangona, V. S., Welsh, R., Chmielewski, G., McInerney, E., Martin, S., . . . Kestin, L. L. (2010). Outcomes after stereotactic lung radiotherapy or wedge resection for stage I non-small-cell lung cancer. *Journal of Clinical Oncology, 28*(6), 928-935. doi: 10.1200/JCO.2009.25.0928

Grimm, J., LaCouture, T., Asbell, S. O., Kramer, N., Pahlajani, N., Ahmad, N., . . . Xue, J. (2012). Evaluating Published Skin Dose Tolerance Limits for Stereotactic Body Radiation Therapy of Lung Cancer. *Cureus, 4*(6), e51. doi: 10.7759/cureus.51

Grimm, J., LaCouture, T., Croce, R., Yeo, I., Zhu, Y., & Xue, J. (2011). Dose tolerance limits and dose volume histogram evaluation for stereotactic body radiotherapy. *Journal of Applied Clinical Medical Physics, 12*(2), 3368. Availabe at: http://jacmp.org/index.php/jacmp/article/viewFile/3368/2170.

Guckenberger, M. (2015). Dose and Fractionation in Stereotactic Body Radiation Therapy for Stage I Non-Small Cell Lung Cancer: Lessons Learned and Where Do We Go Next? *International Journal of Radiation Oncology Biology Physics, 93*(4), 765-768. doi: 10.1016/j.ijrobp.2015.08.025

Guckenberger, M., Allgäuer, M., Appold, S., Dieckmann, K., Ernst, I., Ganswindt, U., . . . Andratschke, N. (2013). Safety and efficacy of stereotactic body radiotherapy for stage 1 non-small-cell lung cancer in routine clinical practice: a patterns-of-care and outcome analysis. *Journal of Thoracic Oncology, 8*(8), 1050-1058. doi: 10.1097/JTO.0b013e318293dc45

Guckenberger, M., Klement, R. J., Allgäuer, M., Appold, S., Dieckmann, K., Ernst, I., . . . Flentje, M. (2013). Applicability of the linear-quadratic formalism for modeling local tumor control probability in high dose per fraction stereotactic body radiotherapy for early stage non-small cell lung cancer. *Radiotherapy and Oncology, 109*(1), 13-20. doi: 10.1016/j.radonc.2013.09.005

Guckenberger, M., Wilbert, J., Krieger, T., Richter, A., Baier, K., Meyer, J., & Flentje, M. (2007). Four-dimensional treatment planning for stereotactic body radiotherapy. *International Journal of Radiation Oncology Biology Physics, 69*(1), 276-285. doi: 10.1016/j.ijrobp.2007.04.074

Guckenberger, M., Wulf, J., Mueller, G., Krieger, T., Baier, K., Gabor, M., . . . Flentje, M. (2009). Dose-response relationship for image-guided stereotactic body radiotherapy of pulmonary tumors: relevance of 4D dose calculation. *International Journal of Radiation Oncology Biology Physics, 74*(1), 47-54. doi: 10.1016/ j.ijrobp.2008.06.1939

Hagan, M. P., Yacoub, A., Grant, S., & Dent, P. (2005). The cellular signaling response to radiation. In B. D. Kavanagh & R. D. Timmerman (Eds.), *Stereotactic body radiation therapy*. Philadelphia, USA: Lippincott Wiliams & Wilkins.

Han, K., Cheung, P., Basran, P. S., Poon, I., Yeung, L., & Lochray, F. (2010). A comparison of two immobilization systems for stereotactic body radiation therapy of lung tumors. *Radiotherapy and Oncology, 95*(1), 103-108. doi: 10.1016/j.radonc.2010.01.025

Haseltine, J. M., Rimner, A., Gelblum, D. Y., Modh, A., Rosenzweig, K. E., Jackson, A., . . . Wu, A. J. (2016). Fatal complications after stereotactic body radiation therapy for central lung tumors abutting the proximal bronchial tree. *Pract Radiat Oncol, 6*(2), e27-33. doi: 10.1016/j.prro.2015.09.012

Hearn, J. W., Videtic, G. M., Djemil, T., & Stephans, K. L. (2014). Salvage stereotactic body radiation therapy (SBRT) for local failure after primary lung SBRT. *International Journal of Radiation Oncology Biology Physics, 90*(2), 402-406. doi: 10.1016/j.ijrobp.2014.05.048

ICRU. (1993). *ICRU report 50: Prescribing, recording and reporting photon beam therapy*: International commission of radiation units and measurements, Bethesda, MD, USA.

ICRU. (1999). *ICRU report 62: Prescribing, recording and reporting photon beam therapy (Supplement to ICRU report 50)*: International commission of radiation units and measurements, Bethesda, MD, USA.

ICRU. (2010). *ICRU report 83: Prescribing, recording and reporting photon-beam intensity-modulated radiation therapy (IMRT)*: International commission of radiation units and measurements. Oxford University Press, Oxford, UK.

Jin, J. Y., Ajlouni, M., Ryu, S., Chen, Q., Li, S., & Movsas, B. (2007). A technique of quantitatively monitoring both respiratory and nonrespiratory motion in patients using external body markers. *Medical Physics, 34*(7), 2875-2881. doi: 10.1118/1.2745237

Joiner, M. C. (2009). Quantifying cell kill and cell survival. In M. Joiner & A. van der Kogel (Eds.), *Basic clinical radiobiology* (4th ed.). Boca Raton, FL, USA: CRC Press.

Josipovic, M., Persson, G. F., Logadottir, A., Smulders, B., Westmann, G., & Bangsgaard, J. P. (2012). Translational and rotational intra- and inter-fractional errors in patient and target position during a short course of frameless stereotactic body radiotherapy. *Acta Oncol, 51*(5), 610-617. doi: 10.3109/0284186X.2011.626448

Karlsson, K., Gagliardi, G., Rutkowska, E., & Lax, I. (2008). SBRT treatments: Reduction of diaphragmatic and tumour excursion by means of forced shallow breathing with abdominal compression. Assessment based on 2504 treated tumours. [Abstract]. *Radiotherapy and Oncology, 88*(S2), S377. Available at: http://www.thegreenjournal.com/article/S0167-8140(08)80054-0/pdf.

Karlsson, K., Nyman, J., Baumann, P., Wersäll, P., Drugge, N., Gagliardi, G., . . . Lax, I. (2013). Retrospective cohort study of bronchial doses and radiation-induced atelectasis after stereotactic body radiation therapy of lung tumors located close to the bronchial tree. *International Journal of Radiation Oncology Biology Physics, 87*(3), 590-595. doi: 10.1016/j.ijrobp.2013.06.2055

Kavanagh, B. D., & Cardinale, R. M. (2005). Special problems in stereotactic body radiation therapy: Dose rate effect, dose inhomogeneity, and target margin selection. In B. D. Kavanagh & R. D. Timmerman (Eds.), *Stereotactic body radiation therapy*. Philadelphia, USA: Lippincott Wiliams & Wilkins.

Keall, P. J., Colvill, E., O'Brien, R., Ng, J. A., Poulsen, P. R., Eade, T., . . . Booth, J. T. (2014). The first clinical implementation of electromagnetic transponder-guided MLC tracking. *Medical Physics, 41*(2), 020702. doi: 10.1118/1.4862509

Kestin, L., Grills, I., Guckenberger, M., Belderbos, J., Hope, A. J., Werner-Wasik, M., . . . Elekta Lung Research, G. (2014). Dose-response relationship with clinical outcome for lung stereotactic body radiotherapy (SBRT) delivered via online image guidance. *Radiotherapy and Oncology, 110*(3), 499-504. doi: 10.1016/j.radonc.2014.02.002

Kirkwood, B., & Sterne, J. (2003). *Essential medical statistics* (2nd ed.). Malden, MA, USA: Blackwell Science Ltd.

Lagerwaard, F. J., Haasbeek, C. J., Smit, E. F., Slotman, B. J., & Senan, S. (2008). Outcomes of risk-adapted fractionated stereotactic radiotherapy for stage I non-small-cell lung cancer. *International Journal of Radiation Oncology Biology Physics, 70*(3), 685-692. doi: 10.1016/j.ijrobp.2007.10.053

Lagerwaard, F. J., Verstegen, N. E., Haasbeek, C. J., Slotman, B. J., Paul, M. A., Smit, E. F., & Senan, S. (2012). Outcomes of stereotactic ablative radiotherapy in patients with potentially operable stage I non-small cell lung cancer. *International Journal of Radiation Oncology Biology Physics, 83*(1), 348-353. doi: 10.1016/j.ijrobp.2011.06.2003

Latifi, K., Oliver, J., Baker, R., Dilling, T. J., Stevens, C. W., Kim, J., . . . Feygelman, V. (2014). Study of 201 non-small cell lung cancer patients given stereotactic ablative radiation therapy shows local control dependence on dose calculation algorithm. *International Journal of Radiation Oncology Biology Physics, 88*(5), 1108-1113. doi: 10.1016/j.ijrobp.2013.12.047

Lax, I. (1993). Target dose versus extratarget dose in stereotactic radiosurgery. *Acta Oncol, 32*(4), 453-457. doi: 10.3109/02841869309093624

Lax, I., & Blomgren, H. (2005). The clinical transition from intracranial to extracranial stereotactic radiation therapy. In B. D. Kavanagh & R. D. Timmerman (Eds.), *Stereotactic body radiation therapy*. Philadelphia, USA: Lippincott Wiliams & Wilkins.

Lax, I., Blomgren, H., Larson, D., & Näslund, I. (1998). Extracranial stereotactic radiosurgery of localized targets. *Journal of Radiosurgery, 1*(2), 135-148. doi: 10.1023/B:JORA.0000010898.87146.2e

Lax, I., Blomgren, H., Näslund, I., & Svanström, R. (1994). Stereotactic radiotherapy of malignancies in the abdomen. Methodological aspects. *Acta Oncol, 33*(6), 677-683. doi: 10.3109/02841869409121782

Leksell, L. (1983). Stereotactic radiosurgery. *J Neurol Neurosurg Psychiatry, 46*(9), 797-803. Available at: http://www.ncbi.nlm.nih.gov/pmc/articles/PMC1027560/pdf/jnnpsyc1000137-1020005.pdf.

Lindberg, K., Grozman, V., Lindberg, S., Lax, I., Lewensohn, R., & Wersäll, P. (2015). Radiation induced brachial plexus toxicity after SBRT of apically located lung lesions. *Radiotherapy and Oncology, 115*, S324-S325. doi: 10.1016/S0167-8140(15)40657-7

Lindberg, K., Nyman, J., Riesenfeld Källskog, V., Høyer, M., Lund, J. A., Lax, I., . . . Lewensohn, R. (2015). Long-term results of a prospective phase II trial of medically inoperable stage I NSCLC treated with SBRT - the Nordic experience. *Acta Oncol, 54*(8), 1096-1104. doi: 10.3109/0284186X.2015.1020966

Lujan, A. E., Larsen, E. W., Balter, J. M., & Ten Haken, R. K. (1999). A method for incorporating organ motion due to breathing into 3D dose calculations. *Medical Physics, 26*(5), 715-720. doi: 10.1118/1.598577

Malaise, E. P., Fertil, B., Chavaudra, N., & Guichard, M. (1986). Distribution of radiation sensitivities for human tumor cells of specific histological types: comparison of in vitro to in vivo data. *International Journal of Radiation Oncology Biology Physics, 12*(4), 617-624. doi: 10.1016/0360-3016(86)90071-4

Mantel, F., Flentje, M., & Guckenberger, M. (2013). Stereotactic body radiation therapy in the re-irradiation situation--a review. *Radiation Oncology, 8*, 7. doi: 10.1186/1748-717X-8-7

Mayles, P., & Williams, P. (2007). Megavoltage photon beams. In P. Mayles, A. Nahum & J.-C. Rosenwald (Eds.), *Handbook of radiotherapy physics - Theory and practice*. Boca Raton, FL, USA: CRC Press Taylor & Francis Group.

McCowan, P. M., Van Uytven, E., Van Beek, T., Asuni, G., & McCurdy, B. M. (2015). An in vivo dose verification method for SBRT-VMAT delivery using the EPID. *Medical Physics, 42*(12), 6955-6963. doi: 10.1118/1.4935201

McKenzie, A., Coffey, M., Greener, T., Hall, C., van Herk, M., Mijnheer, B., & Harrison, A. (2003). Technical overview of geometric uncertainties in radiotherapy. In. (Ed.), *Geometric uncertainties in radiotherapy - Defining the planning target volume*. London, UK: The British Institute of Radiology.

Meijneke, T. R., Petit, S. F., Wentzler, D., Hoogeman, M., & Nuyttens, J. J. (2013). Reirradiation and stereotactic radiotherapy for tumors in the lung: dose summation and toxicity. *Radiotherapy and Oncology, 107*(3), 423-427. doi: 10.1016/j.radonc.2013.03.015

Menten, M. J., Fast, M. F., Nill, S., Kamerling, C. P., McDonald, F., & Oelfke, U. (2016). Lung stereotactic body radiotherapy with an MR-linac - Quantifying the impact of the magnetic field and real-time tumor tracking. *Radiotherapy and Oncology, 119*(3), 461-466. doi: 10.1016/j.radonc.2016.04.019

Mexner, V., Wolthaus, J., Nijkamp, J., van Herk, M., Damen, E., & Sonke, J. (2007). Effects of respiration-induced anatomy variations on dose distributions [abstract]. *Radiotherapy and Oncology, 84*(Suppl. 1), S75. Available at: http://www.thegreenjournal.com/article/S0167-8140(0107)80275-80271/pdf.

Moore, J. A., Gordon, J. J., Anscher, M., Silva, J., & Siebers, J. V. (2012). Comparisons of treatment optimization directly incorporating systematic patient setup uncertainty

with a margin-based approach. *Medical Physics, 39*(2), 1102-1111. doi: 10.1118/1.3679856

Nagata, Y., Takayama, K., Matsuo, Y., Norihisa, Y., Mizowaki, T., Sakamoto, T., . . . Hiraoka, M. (2005). Clinical outcomes of a phase I/II study of 48 Gy of stereotactic body radiotherapy in 4 fractions for primary lung cancer using a stereotactic body frame. *International Journal of Radiation Oncology Biology Physics, 63*(5), 1427-1431. doi: 10.1016/j.ijrobp.2005.05.034

Nahum, A. (2007). Interactions of charged particles with matter. In P. Mayles, A. Nahum & J.-C. Rosenwald (Eds.), *Handbook of radiotherapy physics - Theory and practice*. Boca Raton, FL, USA: CRC Press Taylor & Francis Group.

National Cancer Institute. (2010). Common terminology criteria for adverse events (CTCAE) version 4.0. U.S. Department of health and human services. Available at: http://evs.nci.nih.gov/ftp1/CTCAE/CTCAE_4.03_2010-06-14_QuickReference_8.5x11.pdf.

Nias, A. H. W. (2000). *An introduction to radiobiology* (2nd ed.). Chichester, England: Whiley.

Nielsen, T. B., Hansen, C. R., Westberg, J., Hansen, O., & Brink, C. (2016). Impact of 4D image quality on the accuracy of target definition. *Australasian Physical and Engineering Science in Medicine, 39*(1), 103-112. doi: 10.1007/s13246-015-0400-3

Nikjoo, H., Uehara, S., & Emfietzoglou, D. (2012). Chapter 7: Interaction of photons with matter. Chapter 8: Interaction of electrons with matter. Chapter 12: Cross sections for interactions of photons with matter. *Interaction of radiation with matter*: Boca Raton, FL, USA, CRC Press.

Nuyttens, J. J., & van de Pol, M. (2012). The CyberKnife radiosurgery system for lung cancer. *Expert Rev Med Devices, 9*(5), 465-475. doi: 10.1586/erd.12.35

Nyman, J., Hallqvist, A., Lund, J., Brustugun, O., Bergman, B., Bergström, P., . . . Lax, I. (2016). SPACE - A randomized study of SBRT vs conventional fractionated radiotherapy in medically inoperable stage I NSCLC. *(personal communication, publication in progress).*

Nyman, J., Johansson, K. A., & Hultén, U. (2006). Stereotactic hypofractionated radiotherapy for stage I non-small cell lung cancer--mature results for medically inoperable patients. *Lung Cancer, 51*(1), 97-103. doi: 10.1016/j.lungcan.2005.08.011

Ojala, J. J., Kapanen, M. K., Hyödynmaa, S. J., Wigren, T. K., & Pitkänen, M. A. (2014). Performance of dose calculation algorithms from three generations in lung SBRT: comparison with full Monte Carlo-based dose distributions. *Journal of Applied Clinical Medical Physics, 15*(2), 4662. doi: 10.1120/jacmp.v15i2.4662

Okunieff, P. (2005). Radiation effects and the role of cytokines: Mechanisms and potential clinical implications. In B. D. Kavanagh & R. D. Timmerman (Eds.), *Stereotactic body radiation therapy*. Philadelphia, USA: Lippincott Wiliams & Wilkins.

Onishi, H., Araki, T., Shirato, H., Nagata, Y., Hiraoka, M., Gomi, K., . . . Yamada, K. (2004). Stereotactic hypofractionated high-dose irradiation for stage I nonsmall cell lung carcinoma: clinical outcomes in 245 subjects in a Japanese multiinstitutional study. *Cancer, 101*(7), 1623-1631. doi: 10.1002/cncr.20539

Onishi, H., Shirato, H., Nagata, Y., Hiraoka, M., Fujino, M., Gomi, K., . . . Araki, T. (2011). Stereotactic body radiotherapy (SBRT) for operable stage I non-small-cell lung

cancer: can SBRT be comparable to surgery? *International Journal of Radiation Oncology Biology Physics, 81*(5), 1352-1358. doi: 10.1016/j.ijrobp.2009.07.1751

Palma, D., Visser, O., Lagerwaard, F. J., Belderbos, J., Slotman, B. J., & Senan, S. (2010). Impact of introducing stereotactic lung radiotherapy for elderly patients with stage I non-small-cell lung cancer: a population-based time-trend analysis. *Journal of Clinical Oncology, 28*(35), 5153-5159. doi: 10.1200/JCO.2010.30.0731

Papiez, L., Moskvin, V., & Timmerman, R. D. (2005). Dosimetry of stereotactic body radiation therapy. In B. D. Kavanagh & R. D. TImmerman (Eds.), *Stereotactic body radiation therapy*. Philadelphia, USA: Lippincott Wiliams & Wilkins.

Park, C., Papiez, L., Zhang, S., Story, M., & Timmerman, R. D. (2008). Universal survival curve and single fraction equivalent dose: useful tools in understanding potency of ablative radiotherapy. *International Journal of Radiation Oncology Biology Physics, 70*(3), 847-852. doi: 10.1016/j.ijrobp.2007.10.059

Patel, N. R., Lanciano, R., Sura, K., Yang, J., Lamond, J., Feng, J., . . . Brady, L. (2015). Stereotactic body radiotherapy for re-irradiation of lung cancer recurrence with lower biological effective doses. *J Radiat Oncol, 4*(1), 65-70. doi: 10.1007/s13566-014-0175-2

Peulen, H., Belderbos, J., Guckenberger, M., Hope, A., Grills, I., van Herk, M., & Sonke, J. J. (2015). Target delineation variability and corresponding margins of peripheral early stage NSCLC treated with stereotactic body radiotherapy. *Radiotherapy and Oncology, 114*(3), 361-366. doi: 10.1016/j.radonc.2015.02.011

Peulen, H., Belderbos, J., Rossi, M., & Sonke, J. J. (2014). Mid-ventilation based PTV margins in Stereotactic Body Radiotherapy (SBRT): a clinical evaluation. *Radiotherapy and Oncology, 110*(3), 511-516. doi: 10.1016/j.radonc.2014.01.010

Peulen, H., Karlsson, K., Lindberg, K., Tullgren, O., Baumann, P., Lax, I., . . . Wersall, P. (2011). Toxicity after reirradiation of pulmonary tumours with stereotactic body radiotherapy. *Radiotherapy and Oncology, 101*(2), 260-266. doi: 10.1016/j.radonc.2011.09.012

Poulsen, P. R., Schmidt, M. L., Keall, P., Worm, E. S., Fledelius, W., & Hoffmann, L. (2012). A method of dose reconstruction for moving targets compatible with dynamic treatments. *Medical Physics, 39*(10), 6237-6246. doi: 10.1118/1.4754297

Regionala Cancercentrum i Samverkan. (2015). *Lungcancer - Årsrapport från Nationella lungcancerregistret (NLCR) 2014*. Uppsala, Sweden. Available at: https://www.cancercentrum.se/globalassets/cancerdiagnoser/lunga-och-lungsack/kvalitetsregister/rapport/nlcr_2014_150930.pdf.

Senthi, S., Haasbeek, C. J., Slotman, B. J., & Senan, S. (2013). Outcomes of stereotactic ablative radiotherapy for central lung tumours: a systematic review. *Radiotherapy and Oncology, 106*(3), 276-282. doi: 10.1016/j.radonc.2013.01.004

Seppenwoolde, Y., Shirato, H., Kitamura, K., Shimizu, S., van Herk, M., Lebesque, J. V., & Miyasaka, K. (2002). Precise and real-time measurement of 3D tumor motion in lung due to breathing and heartbeat, measured during radiotherapy. *International Journal of Radiation Oncology Biology Physics, 53*(4), 822-834. doi: 10.1016/S0360-3016(02)02803-1

Shah, C., Kestin, L. L., Hope, A. J., Bissonnette, J. P., Guckenberger, M., Xiao, Y., . . . Grills, I. S. (2013). Required target margins for image-guided lung SBRT: Assessment of

target position intrafraction and correction residuals. *Pract Radiat Oncol, 3*(1), 67-73. doi: 10.1016/j.prro.2012.03.004

Shaverdian, N., Tenn, S., Veruttipong, D., Wang, J., Hegde, J., Lee, C., . . . Lee, P. (2016). The significance of PTV dose coverage on cancer control outcomes in early stage non-small cell lung cancer patients treated with highly ablative stereotactic body radiation therapy. *British Journal of Radiology, 89*(1059), 20150963. doi: 10.1259/bjr.20150963

Shibamoto, Y., Hashizume, C., Baba, F., Ayakawa, S., Manabe, Y., Nagai, A., . . . Ishikura, S. (2012). Stereotactic body radiotherapy using a radiobiology-based regimen for stage I nonsmall cell lung cancer: a multicenter study. *Cancer, 118*(8), 2078-2084. doi: 10.1002/cncr.26470

Shibamoto, Y., Hashizume, C., Baba, F., Ayakawa, S., Miyakawa, A., Murai, T., . . . Asai, R. (2015). Stereotactic body radiotherapy using a radiobiology-based regimen for stage I non-small-cell lung cancer: five-year mature results. *Journal of Thoracic Oncology, 10*(6), 960-964. doi: 10.1097/JTO.0000000000000525

Shirata, Y., Jingu, K., Koto, M., Kubozono, M., Takeda, K., Sugawara, T., . . . Matsushita, H. (2012). Prognostic factors for local control of stage I non-small cell lung cancer in stereotactic radiotherapy: a retrospective analysis. *Radiation Oncology, 7*, 182. doi: 10.1186/1748-717X-7-182

Skiöld, S., Azimzadeh, O., Merl-Pham, J., Näslund, I., Wersäll, P., Lidbrink, E., . . . Haghdoost, S. (2015). Unique proteomic signature for radiation sensitive patients; a comparative study between normo-sensitive and radiation sensitive breast cancer patients. *Mutat Res, 776*, 128-135. doi: 10.1016/j.mrfmmm.2014.12.002

Socialstyrelsen. (2015). *Cancerincidens i Sverige 2014 - Nya diagnosticerade cancerfall år 2014*. Sweden. Available at: http://www.socialstyrelsen.se/publikationer2015/2015-12-26.

Socialstyrelsen, & Cancerfonden. (2013). *Cancer i siffror 2013 - Populärvetenskapliga fakta om cancer*. Sweden. Available at: http://www.socialstyrelsen.se/ publikationer2013/2013-6-5.

Sonke, J. J., Rossi, M., Wolthaus, J., van Herk, M., Damen, E., & Belderbos, J. (2009). Frameless stereotactic body raditherapy for lung cancer using four-dimensional cone beam CT guidance. *International Journal of Radiation Oncology Biology Physics, 74*(2), 567-574. doi: 10.1016/j.ijrobp.2008.08.004

Steel, G. (2007). Radiobiology of normal tissues. In P. Mayles, A. Nahum & J.-C. Rosenwald (Eds.), *Handbook of radiotherapy physics - Theory and practice*. Boca Raton, FL, USA: CRC Press Taylor & Francis Group.

Steel, G., Chapman, D., & Nahum, A. (2007). Radiobiology of tumours. In P. Mayles, A. Nahum & J.-C. Rosenwald (Eds.), *Handbook of radiotherapy physics - Theory and practice*. Boca Raton, FL, USA: CRC Press Taylor & Francis Group.

Steel, G., & Nahum, A. (2007). Dose fractionation in radiotherapy. In P. Mayles, A. Nahum & J.-C. Rosenwald (Eds.), *Handbook of radiotherapy physics - Theory and practice*. Boca Raton, FL, USA: CRC Press Taylor & Francis Group.

Steenbakkers, R., Duppen, J. C., Fitton, I., Deurloo, K. E. I., Zijp, L. J., Comans, E. F. I., . . . Rasch, C. R. N. (2006). Reduction of observer variation using matched CT-PET for lung cancer delineation: A three-dimensional analysis. *International Journal of*

Radiation Oncology Biology Physics, 64(2), 435-448. doi: 10.1016/ j.ijrobp.2005.06.034

Stroom, J. C., de Boer, H. C. J., Huizenga, H., & Visser, A. G. (1999). Inclusion of geometrical uncertainties in radiotherapy treatment planning by means of coverage probability. *International Journal of Radiation Oncology Biology Physics, 43*(4), 905-919. doi: 10.1016/s0360-3016(98)00468-4

Sweeney, R. A., Seubert, B., Stark, S., Homann, V., Muller, G., Flentje, M., & Guckenberger, M. (2012). Accuracy and inter-observer variability of 3D versus 4D cone-beam CT based image-guidance in SBRT for lung tumors. *Radiation Oncology, 7*, 81. doi: 10.1186/1748-717X-7-81

Tatekawa, K., Iwata, H., Kawaguchi, T., Ishikura, S., Baba, F., Otsuka, S., . . . Shibamoto, Y. (2014). Changes in volume of stage I non-small-cell lung cancer during stereotactic body radiotherapy. *Radiation Oncology, 9*, 8. doi: 10.1186/1748-717X-9-8

Thames, H. D., & Hendry, J. H. (1987). *Fractionation in radiotherapy*. Basingstoke, Hants, Great Britain: Taylor & Francis.

Therasse, P., Arbuck, S. G., Eisenhauer, E. A., Wanders, J., Kaplan, R. S., Rubinstein, L., . . . Gwyther, S. G. (2000). New guidelines to evaluate the response to treatment in solid tumors. *J Natl Cancer Inst, 92*(3), 205-216. doi: 10.1093/jnci/92.3.205

Tilly, D., & Ahnesjö, A. (2015). Fast dose algorithm for generation of dose coverage probability for robustness analysis of fractionated radiotherapy. *Physics in Medicine and Biology, 60*(14), 5439-5454. doi: 10.1088/0031-9155/60/14/5439

Timmerman, R. D., Hu, C., Michalski, J., Straube, W., Galvin, J., Johnstone, D., . . . Choy, H. (2014). Long-term Results of RTOG 0236: A Phase II Trial of Stereotactic Body Radiation Therapy (SBRT) in the Treatment of Patients with Medically Inoperable Stage I Non-Small Cell Lung Cancer. *International Journal of Radiation Oncology Biology Physics, 90*, S30-S30. doi: 10.1016/j.ijrobp.2014.05.135

Timmerman, R. D., & Lohr, F. (2005). Normal tissue dose constraints applied in lung stereotactic body radiation therapy. In B. D. Kavanagh & R. D. Timmerman (Eds.), *Stereotactic body radiation therapy*. Philadelphia, USA: Lippincott Wiliams & Wilkins.

Timmerman, R. D., McGarry, R., Yiannoutsos, C., Papiez, L., Tudor, K., DeLuca, J., . . . Fletcher, J. (2006). Excessive toxicity when treating central tumors in a phase II study of stereotactic body radiation therapy for medically inoperable early-stage lung cancer. *Journal of Clinical Oncology, 24*(30), 4833-4839. doi: 10.1200/JCO.2006.07.5937

Timmerman, R. D., Pass, H., Galvin, J., Edelman, M. J., Gore, E., Kong, F.-M. S. P., & Hu, C. (2014). A phase II trial of stereotactic body radiation therapy (SBRT) in the treatment of patients with operable stage I/II non-small cell lung cancer: Radiation Therapy Oncology Group 0618. Available at: http://www.rtog.org.

Timmerman, R. D., Paulus, R., Galvin, J., Michalski, J., Straube, W., Bradley, J., . . . Choy, H. (2009). Stereotactic Body Radiation Therapy for Medically Inoperable Early-stage Lung Cancer Patients: Analysis of RTOG 0236. *International Journal of Radiation Oncology Biology Physics, 75*(3), S3-S3. doi: 10.1016/j.ijrobp.2009.07.033

Timmerman, R. D., Paulus, R., Pass, H. I., Gore, E., Edelman, M. J., Galvin, J. M., . . . Bradley, J. D. (2013). RTOG 0618: Stereotactic body radiation therapy (SBRT) to

treat operable early-stage lung cancer patients. *Journal of Clinical Oncology, 31*, Abstract 7523. Available at: http://meetinglibrary.asco.org/content/111599-111132.

van Baardwijk, A., Tomé, W. A., van Elmpt, W., Bentzen, S. M., Reymen, B., Wanders, R., . . . De Ruysscher, D. (2012). Is high-dose stereotactic body radiotherapy (SBRT) for stage I non-small cell lung cancer (NSCLC) overkill? A systematic review. *Radiotherapy and Oncology, 105*(2), 145-149. doi: 10.1016/j.radonc.2012.09.008

van der Voort van Zyp, N. C., Prevost, J. B., van der Holt, B., Braat, C., van Klaveren, R. J., Pattynama, P. M., . . . Nuyttens, J. J. (2010). Quality of life after stereotactic radiotherapy for stage I non-small-cell lung cancer. *International Journal of Radiation Oncology Biology Physics, 77*(1), 31-37. doi: 10.1016/j.ijrobp.2009.04.080

van Herk, M., Remeijer, P., Rasch, C., & Lebesque, J. V. (2000). The probability of correct target dosage: dose-population histograms for deriving treatment margins in radiotherapy. *International Journal of Radiation Oncology Biology Physics, 47*(4), 1121-1135. doi: 10.1016/S0360-3016(00)00518-6

van Herk, M., Witte, M., van der Geer, J., Schneider, C., & Lebesque, J. V. (2003). Biologic and physical fractionation effects of random geometric errors. *International Journal of Radiation Oncology Biology Physics, 57*(5), 1460-1471. doi: 10.1016/j.ijrobp.2003.08.026

Wennberg, B., & Lax, I. (2013). The impact of fractionation in SBRT: analysis with the linear quadratic model and the universal survival curve model. *Acta Oncol, 52*(5), 902-909. doi: 10.3109/0284186X.2012.728292

Verellen, D., De Ridder, M., Linthout, N., Tournel, K., Soete, G., & Storme, G. (2007). Innovations in image-guided radiotherapy. *Nature Reviews Cancer, 7*(12), 949-960. doi: 10.1038/nrc2288

Verellen, D., Depuydt, T., Gevaert, T., Linthout, N., Tournel, K., Duchateau, M., . . . De Ridder, M. (2010). Gating and tracking, 4D in thoracic tumours. *Cancer Radiotherapie, 14*(6-7), 446-454. doi: 10.1016/j.canrad.2010.06.002

Videtic, G. M., Hu, C., Singh, A. K., Chang, J. Y., Parker, W., Olivier, K. R., . . . Choy, H. (2015). A Randomized Phase 2 Study Comparing 2 Stereotactic Body Radiation Therapy Schedules for Medically Inoperable Patients With Stage I Peripheral Non-Small Cell Lung Cancer: NRG Oncology RTOG 0915 (NCCTG N0927). *International Journal of Radiation Oncology Biology Physics, 93*(4), 757-764. doi: 10.1016/j.ijrobp.2015.07.2260

Videtic, G. M., Singh, A. K., Chang, J. Y., Le, Q., Parker, W., Olivier, K. R., . . . Hu, C. (2014). A randomized phase II study comparing 2 stereotactic body radiation therapy (SBRT) schedules for medically inoperable patients with stage I peripheral non-small cell lung cancer: Radiation Therapy Oncology Group 0915. Available at: http://www.rtog.org.

Williams, J. R., Zhang, Y., Zhou, H., Gridley, D. S., Koch, C. J., Russell, J., . . . Little, J. B. (2008). A quantitative overview of radiosensitivity of human tumor cells across histological type and TP53 status. *Int J Radiat Biol, 84*(4), 253-264. doi: 10.1080/09553000801953342

Witte, M. G., van der Geer, J., Schneider, C., Lebesque, J. V., & van Herk, M. (2004). The effects of target size and tissue density on the minimum margin required for random errors. *Medical Physics, 31*(11), 3068-3079. doi: 10.1118/1.1809991

Wolthaus, J. W., Schneider, C., Sonke, J. J., van Herk, M., Belderbos, J. S., Rossi, M. M., . . . Damen, E. M. (2006). Mid-ventilation CT scan construction from four-dimensional respiration-correlated CT scans for radiotherapy planning of lung cancer patients. *International Journal of Radiation Oncology Biology Physics, 65*(5), 1560-1571. doi: 10.1016/j.ijrobp.2006.04.031

Wolthaus, J. W., Sonke, J. J., van Herk, M., Belderbos, J. S., Rossi, M. M., Lebesque, J. V., & Damen, E. M. (2008). Comparison of different strategies to use four-dimensional computed tomography in treatment planning for lung cancer patients. *International Journal of Radiation Oncology Biology Physics, 70*(4), 1229-1238. doi: 10.1016/j.ijrobp.2007.11.042

Worm, E. S., Hansen, A. T., Petersen, J. B., Muren, L. P., Praestegaard, L. H., & Høyer, M. (2010). Inter- and intrafractional localisation errors in cone-beam CT guided stereotactic radiation therapy of tumours in the liver and lung. *Acta Oncol, 49*(7), 1177-1183. doi: 10.3109/0284186X.2010.498435

Wouters, B. G., & Begg, A. C. (2009). Irradiation-induced damage and the DNA damage response. In M. Joiner & A. van der Kogel (Eds.), *Basic clinical radiobiology* (4th ed.). Boca Raton, FL, USA: CRC Press.

Wulf, J., Baier, K., Mueller, G., & Flentje, M. P. (2005). Dose-response in stereotactic irradiation of lung tumors. *Radiotherapy and Oncology, 77*(1), 83-87. doi: 10.1016/j.radonc.2005.09.003

Wulf, J., Haedinger, U., Oppitz, U., Thiele, W., Mueller, G., & Flentje, M. (2004). Stereotactic radiotherapy for primary lung cancer and pulmonary metastases: a noninvasive treatment approach in medically inoperable patients. *International Journal of Radiation Oncology Biology Physics, 60*(1), 186-196. doi: 10.1016/j.ijrobp.2004.02.060

Wunderink, W., Mendez Romero, A., de Kruijf, W., de Boer, H., Levendag, P., & Heijmen, B. (2008). Reduction of respiratory liver tumor motion by abdominal compression in stereotactic body frame, analyzed by tracking fiducial markers implanted in liver. *International Journal of Radiation Oncology Biology Physics, 71*(3), 907-915. doi: 10.1016/j.ijrobp.2008.03.010

Yan, D., Lockman, D., Martinez, A., Wong, J., Brabbins, D., Vicini, F., . . . Kestin, L. (2005). Computed tomography guided management of interfractional patient variation. *Seminars in Radiation Oncology, 15*(3), 168-179. doi: 10.1016/j.semradonc.2005.01.007

Zhang, J., Yang, F., Li, B., Li, H., Liu, J., Huang, W., . . . Wang, J. (2011). Which is the optimal biologically effective dose of stereotactic body radiotherapy for Stage I non-small-cell lung cancer? A meta-analysis. *International Journal of Radiation Oncology Biology Physics, 81*(4), e305-316. doi: 10.1016/j.ijrobp.2011.04.034

Zhao, L., Balter, P., Gomez, D. R., Welsh, J. W., Lin, S. H., & Chang, J. Y. (2015). What is the optimal SABA dose for local control after stereotactic ablative radiation therapy in lung cancer: a 10 year experience of 1092 patients. *International Journal of Radiation Oncology Biology Physics, 93*(3), E390-E390. doi: 10.1016/j.ijrobp.2015.07.1542

Zimmermann, F. B., Geinitz, H., Schill, S., Thamm, R., Nieder, C., Schratzenstaller, U., & Molls, M. (2006). Stereotactic hypofractionated radiotherapy in stage I (T1-2 N0 M0) non-small-cell lung cancer (NSCLC). *Acta Oncol, 45*(7), 796-801. doi: 10.1080/02841860600913210